PJNM

Philippine Journal of Nuclear Medicine

Vol. 18 No. 2 July to December 2023

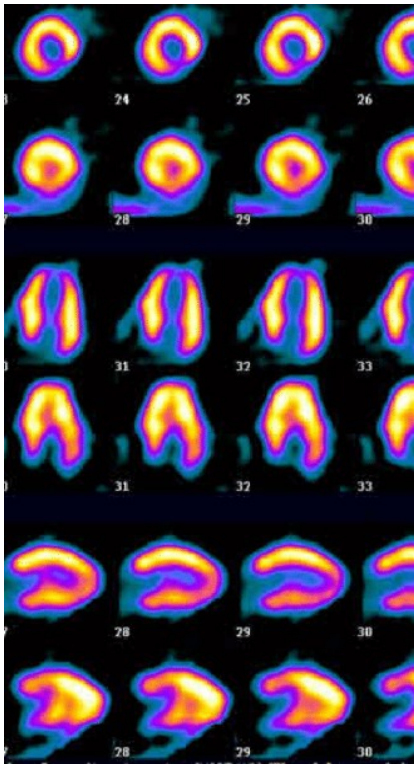

Contents:

Philippine Journal of Nuclear Medicine

Volume 18 No. 2
July to December 2023

Official Publication of the Philippine Society of Nuclear Medicine

The Philippine Journal of Nuclear Medicine is a peer-reviewed journal published by the Philippine Society of Nuclear Medicine. Subscription is free to all PSNM members in good standing as part of their membership privileges.

The Journal will be primarily of interest to medical and paramedical personnel working in nuclear medicine and related fields. Original works in clinical nuclear medicine and allied disciplines in physics, dosimetry, radiation biology, computer science, radiopharmacy, and radiochemistry are welcome. Review articles are usually solicited and published together with related reviews. Case reports of outstanding interest are likewise welcome. PSNM documents and position papers of interest to the reader will also be published as necessary.

Manuscripts for consideration should be sent to:

The Editor, Vincent Peter C. Magboo, MD
Philippine Journal of Nuclear Medicine
c/o Philippine Society of Nuclear Medicine
Unit 209 One Beatriz Tower Condo
4 Lauan St. cor. Aurora Blvd
Project 3, Quezon City 1102, Philippines
Contact. No.: +63 (966) 976 5676
Email: vcmagboo@up.edu.ph
philnucmed@gmail.com

All business communications and requests for complimentary copies should be addressed to the above.

ISSN 1655-9266

INFORMATION FOR AUTHORS

EDITORIAL POLICY

The Philippine Journal of Nuclear Medicine is the official peer-reviewed publication of the Philippine Society of Nuclear Medicine. The Journal accepts original articles pertinent to the field of nuclear medicine. Articles may be on any of the following: clinical and basic sciences, case reports, technical notes, special contributions, and editorials.

Submission of manuscripts

The submitted manuscript package should consist of: (1) the full text (including tables) in Microsoft Word, plain text or ConTeXt document format; and (2) high-resolution JPEG files of all images used in the manuscript. The complete manuscript package may be submitted as a compressed (.ZIP) file by email to philnucmed@gmail.com, or in an optical disc (CD/DVD) and mailed to

> The Editor: Philippine Journal of Nuclear Medicine, c/o Philippine Society of Nuclear Medicine, Unit 209 One Beatriz Tower Condo, 4 Lauan St. cor. Aurora Blvd., Project 3, Quezon City 1102, Philippines.

Manuscripts should be accompanied by a cover letter signed by the author responsible for correspondence regarding the manuscript. The cover letter should contain the following statement:

"All copyright ownership is transferred to the Philippine Journal of Nuclear Medicine upon acceptance of the article _____. This manuscript has been seen and approved by all the authors. The authors stipulate that the material submitted to the Philippine Journal of Nuclear Medicine is an original work and has not been submitted to another publication for concurrent consideration. Any human and/or animal studies undertaken as part of the research are in compliance with regulations of our in stitution(s) and with generally accepted guidelines governing such work."

The cover letter should also give any additional information that may be helpful to the Editor. Signed cover letters sent by email should be in PDF format.

MANUSCRIPT FORMAT

Manuscripts must be written in English, and printed on letter-sized white bond paper, 8.5 in x 11 in (21.6 cm x 27.9 cm). The text should be on one side of the paper only, single-spaced, with at least 1.5 in (4 cm) margins on all sides. Each of the following sections must begin on separate pages and in the following order: title page, abstract, text, acknowledgments, references, tables (each on a separate page), and legends. Pages should be consecutively numbered beginning with the title page. The first line of paragraphs should be indented by at least five spaces.

Title page

The title page should include: (1) a concise but informative title; (2) a short running head or footline of no more than 40 characters; (3) a complete byline, with first name, middle initial, and last name of each author and highest adacemic degrees; (4) the complete affiliation for each author, with the name of departments and institutions to which the work should be attributed; (5) disclaimers, if any; (6) the name, address, and telephone number of the author responsible for correspondence about the manuscript; and (7) the name and address of author to whom reprint requests should be directed.

Abstract and key words
An abstract of no more than 300 words should state the purpose of the study or investigation, summary of methodology, major findings, and principal conclusions. New and important aspects of the study or observations should be emphasized. No figures, abbreviations or reference citations are to be used in the abstract.

Text

The text of original scientific and technical articles is usually divided into the following sections: Introduction, Materials and Methods, Results, Discussion, and Summary or Conclusion.

Case reports are divided into the following sections: Introduction, Case Report, Discussion, and Conclusion. They should contain a concise description of one to three patients, emphasizing the nuclear medicine aspects and include methodology, data and correlative studies. Procedures should be described in sufficient detail to allow other investigators to reproduce the results.

Other articles, e.g. review articles, position papers, or editorials, should introduce a problem or question, present evidence, and conclude with an answer. Generally, review articles should have extensive documentation. Literature citations should represent the breadth and depth of the subjects being reviewed. The organization of review articles will depend greatly on the subject matter and material.

Generic names must be used throughout the text. Instruments and radiopharmaceuticals must be identified by manufacturer name and address in parentheses.

Acknowledgments

Persons or agencies contributing substantially to the work, including any grant support, must be acknowledged.

References

References must be cited in consecutive numerical order at first mention in the text and designated by the reference number in parentheses. References appearing in a table or figure should be numbered sequentially with those in the text.

The reference list must be numbered consecutively as in the text. The journal follows Index Medicus style for references and abbreviates journal names according to the List of Journals Indexed in Index Medicus. 'Unpublished observations' and 'personal communications' should not be used as references, although written—not verbal—communications may be noted as such in the text. The author is responsible for the accuracy of all references and must verify them against the original document.

For journal articles with six or less authors, all authors must be listed. For those with seven or more authors, only the first three are listed, and "et al." is added to the end of the list.

> Seabold JE, Conrad GR, Kimball DA, Ponto JA and Cricker JA. Pitfalls in establishing the diagnosis of deep venous thrombophlebitis by indium-111 platelet scintigraphy. J Nucl Med 1988;29:1169–1180.

For book and book chapters:

> Williams LJ. Evaluation of parathyroid function. In: Brock LJ, Stein JB, eds. The parathyroid and its diseases. 4th ed. New York: Wiley; 1985:196–248.
>
> Goodyear B. Bone marrow transplantation in severe combined immunodeficiency syndrome. In: Gree HJ, Blackscmith R, eds. Proceedings of the fourth biennial meeting of the International Society of Transplantation. Houston: International Society of Transplantation; 174: 44–46.

For journal article in electronic format:

> Author. Title. Journal name. Online publishing date. Available from: URL address.

Tables

Each table should be typed double-spaced on a separate page. Do not submit tables as photographs. Tables should be self-explanatory and should supplement, not duplicate, the text. Each table must be cited in consecutive numerical order in the text. Tables should be numbered consecutively with a Roman number following the word TABLE.

Illustrations

Illustrations should clarify and augment the text. Figures should be sharp and of high quality. Glossy photographs of line drawings rendered professionally on white drawing paper in black India ink, with template or typeset lettering, should be submitted. High quality computer-generated art is also acceptable. Letters, numbers, and symbols should be clear and of sufficient size to retain legibility after reduction.

Each illustration must be numbered and cited in consecutive order in the text. Illustrations should be identified on a gummed label. Legends should be typed double-spaced on a separate page. Figures should be numbered with an Arabic number following the word FIGURE.

Units of measurement

Use of the International System of Units (SI) is standard. Measurements of length, height, weight, and volume must be reported in metric units. Other measurements must be reported in the units in which they were made. Alternative units (non-SI units) should be added in parentheses by the author, if indicated.

Abbreviations and symbols

Only standard abbreviations and symbols should be used in the text. At first mention, the complete term, followed by its abbreviations in parentheses, must be used in the text. Standard units of measure should not be expanded at first mention. Consult a style manual, if necessary.

REVIEW PROCEDURE

Submitted manuscripts are peer-reviewed for originality, significance, adequacy of documentation, reader interest, composition, and adherence to the guidelines. Manuscripts are returned to the author for revision if suggestions and criticisms have been made. All accepted manuscripts are subject to editing for scientific accuracy, clarity, and style.

MedChoice
Thyroid & Diabetes
HEALTHCARE

LEVOTHYROXINE SODIUM

THYDIN

Rx 12.5 mcg • 25 mcg • 50 mcg • 100 mcg • 150 mcg
THYROID HORMONES

METHIMAZOLE

TAPDIN

Rx 5 mg & 20 mg Tablet
ANTITHYROID

PROPRANOLOL HYDROCHLORIDE

INDIRIN

Rx 10 mg & 40 mg Film-Coated Tablet
BETA BLOCKING AGENT, NON-SELECTIVE

CARBIMAZOLE

NEOMERDIN

Rx 5 mg & 20 mg Tablet
ANTITHYROID

MEDCHOICE ENDOCRINE GROUP, INC.
Unit 901-1001, 88 Corporate Center,
Sedeño corner Valero Streets, Salcedo Village, Makati City

www.medchoicepharma.com
www.facebook.com/MedChoicePharmaInc

"FULL PRESCRIBING INFORMATION AND SRP AVAILABLE UPON REQUEST"
Available in Mercury Drug, Watsons Pharmacy, MedExpress Drugstore,
and other leading drugstores nationwide.

MEGI-08-2023/01/19


An established global key player in the **radioisotope & radiopharmaceutical** field.
Find out more about us and our products:
www.itm-radiopharma.com
Follow us:
itm
PASSION FOR PRECISION

Complete and Sustained Response After Peptide Receptor Radionuclide Therapy in a 66-Year-Old Filipino Male with Metastatic Pancreatic Neuroendocrine Tumor: A Case Report

Carl Joshua M. Chianpian, MD, Patricia A. Bautista-Peñalosa, MD, Carl Johnry J. Santos, MD, Irene S. Bandong, MD

Department of Nuclear Medicine and Theranostics, St. Luke's Medical Center, Quezon City
E-mail address: joshchianpian@yahoo.com

ABSTRACT

The introduction of peptide receptor radionuclide therapy (PRRT) to the Philippines has allowed for novel approaches in the management of neuroendocrine tumors (NETs). This case report details the management of a 66-year-old Filipino man diagnosed with metastatic pancreatic NET after biopsy and staging with Ga-68 DOTATATE PET-CT. After poor response to somatostatin analogue therapy, the patient was advised to undergo PRRT. Upon completing four cycles of PRRT with Lu-177 DOTATATE, the metastatic hepatic lesions showed resolution and the pancreatic tail tumor exhibited regression, allowing the patient to undergo surgical resection of the primary tumor. On follow-up, he was declared to be in remission with good quality of life and no imaging evidence of recurrence. The case underscores the diagnostic and therapeutic utility of radiolabeled somatostatin analogues along with the importance of a multidisciplinary approach in the management of an initially unresectable metastatic pancreatic NET

***Keywords**: peptide receptor radionuclide therapy, metastatic pancreatic neuroendocrine tumor, Ga-68 DOTATATE, Lu-177 DOTATATE*

INTRODUCTION

The emergence of novel radiopharmaceuticals for theranostics has launched countless possibilities in the management of various malignancies. Although several radionuclides and biomolecules are presently being studied for the targeted delivery of radiation to tumors of diverse pathologies, the burgeoning era of theranostics has primarily been led by peptide receptor radionuclide therapy (PRRT) for neuroendocrine tumors (NETs), closely trailed by prostate-specific membrane antigen radioligand therapy for metastatic castrate-resistant prostate carcinoma [1].

By exploiting the molecular biology of NETs that overexpress somatostatin receptors (SSTR), PRRT selectively delivers therapeutic doses of radiation to target neuroendocrine tissues using radionuclides, such as Yttrium-90 (Y-90) or Lutetium-177 (Lu-177), attached to somatostatin analogues.[2] Decades of research and development have contributed to the vast literature supporting the use of radiolabeled somatostatin analogues for therapy. From the initial studies using Iodine-123 Tyr3-octreotide (TOCT) in 1987 to the advent of Indium-111 pentetreotide along with Y-90 and Lu-177 tetraazacyclododecanetetraacetic acid (DOTA)-Tyr3-octreotide (DOTATOC) in the 1990s to the first clinical application of Lu-177 DOTA-Tyr3- octreotate (DOTATATE) in 2000,[3] PRRT has undergone significant growth in the preceding decades. This growing bulk of clinical evidence eventually culminated in the NETTER-1 trial, which demonstrated the efficacy of adding PRRT to somatostatin analogue therapy for gastroenteropancreatic (GEP) NETs with a markedly higher response rate and progression-free survival at 20 months compared to somatostatin analogue therapy alone [4]. This was eventually followed by the US FDA approval of Lu-177 DOTATATE (Lutathera) [5] and its integration into the National Comprehensive Cancer Network (NCCN) Clinical Practice Guidelines in Oncology in 2022 as a front-line treatment option for metastatic GEP NETs alongside somatostatin analogue therapy, immunotherapy, cytotoxic chemotherapy, and other local therapies directed to the liver and/or bones [6].

Although much of the existing literature has come from high volume centers in Europe and Oceania, theranostics

has slowly found its foothold in developing countries in recent years. Case reports detailing local experience with PRRT have shown its utility in eliciting response and establishing disease control in various NETs.[7,8] The following case report will delve into the use of PRRT as a neoadjuvant treatment for metastatic pancreatic NET in a tertiary referral institution in the Philippines. The objective of the study is to underscore the growing role of PRRT and SSTR positron emission tomography (PET) - computed tomography (CT) in the management of NETs in the Philippine setting.

CASE REPORT

A 66-year-old Filipino man initially presenting with diarrhea underwent work-up with ultrasound and MRI, which revealed a 2.5 x 3.8 cm mass at the pancreatic tail. Fine needle aspiration biopsy of the aforementioned mass revealed cytomorphologic findings suggestive of a low-grade neoplasm. Immunohistochemical testing showed that the samples were positive for synaptophysin and chromogranin, but negative for anti-trypsin and carbohydrate antigen 19-9, supporting the diagnosis of a pancreatic neuroendocrine neoplasm; however, the paucity of cells in the sample precluded evaluation of the Ki-67 index, which is needed to characterize the degree of tumor differentiation.

In lieu of performing another biopsy, the medical oncologist requested for a Ga-68 DOTATATE PET-CT scan (Figure 1.A), which showed SSTR overexpression in the inhomogeneously enhancing pancreatic tail tumor with a maximum standardized uptake value (SUVmax) of 31.3. The scan also revealed increased DOTATATE uptake in an inhomogeneously enhancing nodule at hepatic segment VI, measuring 2.1 x 2.5 cm, along with several smaller DOTATATE-avid foci in both hepatic lobes, with an SUVmax of up to 38.5. Non-specific DOTATATE uptake was likewise noted in the prostate gland, attributed to benign prostatic hyperplasia. Although the left adrenal gland was nodular on CT, its DOTATATE uptake appeared physiologic. Overall, the SSTR overexpression in the primary pancreatic lesion and hepatic metastases suggested a well-differentiated (WHO grade I) neuroendocrine tumor, and the patient was started on long-acting somatostatin analogue injections.

After four months of somatostatin analogue therapy, a repeat whole body Ga-68 DOTATATE PET-CT scan (Figure 1.B) was requested to evaluate treatment response. The pancreatic tail mass demonstrated a 176.7% interval increase of DOTATATE uptake, now with an SUVmax of 86.6. Slight increase by 8.6% of DOTATATE uptake was also seen in several of the hepatic nodules, with an SUVmax of up to 41.8, with concurrent progression in size and number on CT.

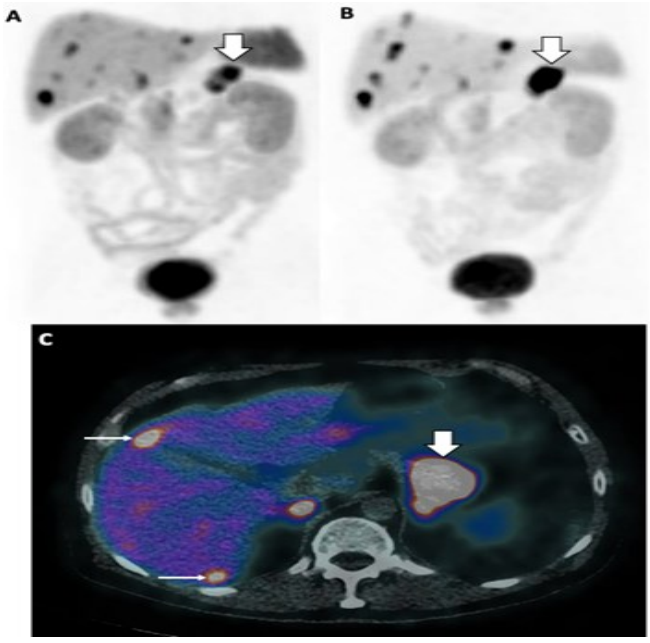

FIGURE 1. Maximum intensity projection (MIP) images of the Ga-68 DOTATATE PET-CT scans on baseline dated September 2018 (A) and after four months of somatostatin analogue therapy dated January 2019 (B) showing interval increase of SSTR expression in the pancreatic tail tumor (thick arrow). Fused PET-CT image (C) shows DOTATATE-avid lesions in the pancreatic tail (thick arrow) and liver (thin arrows).

With evidence of progressive disease based on the Response Evaluation Criteria in Solid Tumors (RECIST) 1.1 after somatostatin analogue therapy, the patient was advised by his Filipino and Singaporean oncologists to undergo PRRT and was referred to the nuclear medicine service. Initial evaluation showed acceptable baseline hematologic, renal, and hepatic functions. The patient then underwent a total of four cycles of PRRT over the course of eight months. In each cycle, anti-emetic and anti-inflammatory medications were given shortly before therapy. Gelofusine was administered for renal protection and adequate hydration was ensured orally and intravenously. A diuretic was given after every therapy to reduce the radiation dose delivered to the kidneys.

On the first cycle of therapy, 6.5 gigabequerels (GBq) of Lu-177 DOTATATE was administered. The 48-hour post-therapy scan showed Lu—177 DOTATATE uptake in the

pancreatic tail tumor and the hepatic metastases, similar to the findings of the prior (January 2019) Ga-68 DOTATATE PET-CT scan. Two months after the first cycle of therapy, the patient underwent a repeat Ga-68 DOTATATE PET-CT scan (Figure 2.A), which demonstrated significant decrease of DOTATATE uptake by 71.6% in the pancreatic tail tumor, now with an SUVmax of 24.6. Resolution of DOTATATE uptake was noted in all of the hepatic metastases with corresponding morphologic regression to resolution, the largest of which measures 1.3 x 1.1 cm.

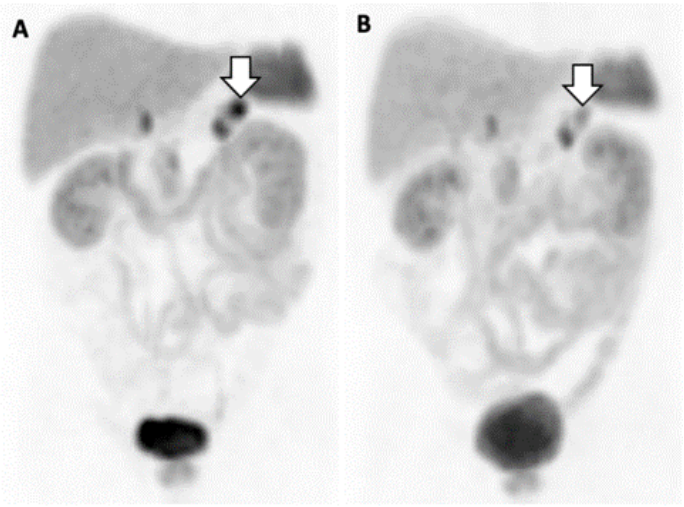

FIGURE 2. Maximum intensity projection (MIP) images of the Ga-68 DOTATATE PET-CT scan after the first cycle dated March 2019 (A) and after the fourth cycle of PRRT dated December 2019 (B). The previously noted DOTATATE-avid hepatic lesions in Figure 1 have resolved after the first cycle, while gradual regression of DOTATATE uptake is seen in the pancreatic tail tumor (thick arrow).

In the absence of clinical or imaging evidence of residual metastatic disease, the patient was referred to a hepatobiliary surgeon for laparoscopic distal pancreatectomy with left adrenalectomy, frozen section biopsy and wedge resection of a liver nodule that was seen intraoperatively. The histopathologic findings reported a low-grade well-differentiated (WHO grade I) pancreatic NET. Immunohistochemical stains were positive for synaptophysin (Figure 3.A), chromogranin (Figure 3.B), and neuron specific enolase (NSE) (Figure 3.C). Ki-67 index (Figure 3.D) was 1.2% and mitotic count was < 2 mitosis/10 hpf, consistent with a well-differentiated pathology. The nodular left adrenal gland was negative for tumor, while the resected liver nodule was shown to be benign hepatic parenchyma with steatosis.

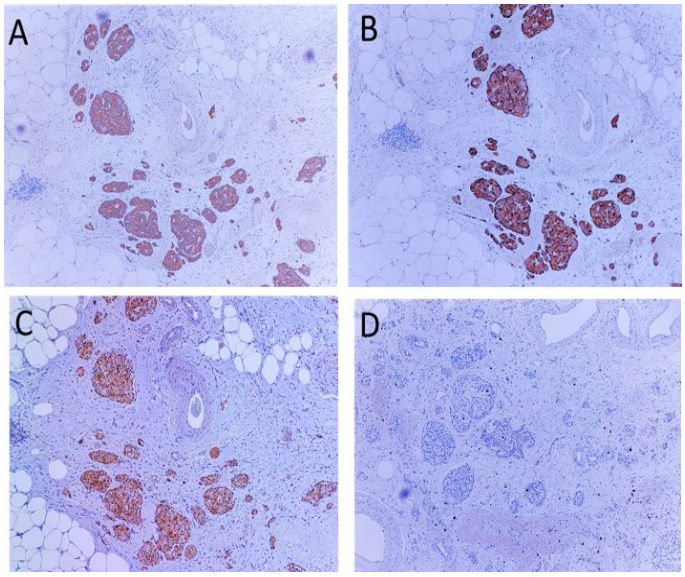

FIGURE 3. Immunohistochemical stains (20x magnification): (A) synaptophysin, (B) chromogranin, (C) neuron specific enolase, and (D) Ki-67

The patient then had his second (6.2 GBq), third (6.7 GBq) and fourth (6.5 GBq) cycles of Lu-177 DOTATATE therapy every three months, which were well-tolerated without impairment of hematologic, renal, and hepatic functions. The post-Lu-177 therapy scans noted decreasing DOTATATE avidity in the pancreatic tail tumor with no new DOTATATE-avid lesions detected. Two months after the fourth cycle of Lu-177 DOTATATE therapy, a repeat Ga-68 DOTATATE PET-CT scan (Figure 2.B) was done for treatment response evaluation. The scan showed further regression of SSTR expression by 52.4% in the stable-sized pancreatic tail tumor, now only with an SUVmax of 11.7. All hepatic nodules have likewise resolved on CT.

On follow-up Ga-68 DOTATATE PET-CT scan (Figure 4) two years after surgery, no tumor recurrence was noted and no SSTR-overexpressing hepatic metastases were seen. There was no hematologic toxicity or nephrotoxicity on follow-up laboratory tests. His initial complaint of diarrhea has resolved. At 54 months since the diagnosis, the patient remains asymptomatic with good social and occupational functions including an Eastern Cooperative Oncology Group (ECOG) performance status of 0.

FIGURE 4. Maximum intensity projection (MIP) image of the Ga-68 DOTATATE PET-CT scan 29 months after the last PRRT dated March 2022, s/p laparoscopic distal pancreatectomy with left adrenalectomy

DISCUSSION

Pancreatic NETs make up about 7% of all NETs and less than 2% of all pancreatic neoplasms. Their incidence is less than 1 case per 100,000 people annually, but it has increased in recent years due to improvement in imaging techniques and diagnosis [9]. The 3-to-5-year survival of pancreatic NET patients without hepatic metastasis is 75-99%, but this drastically drops to 13-54% in the setting of hepatic metastasis [10].

Nuclear medicine has long been involved in the management of NETs; however, for several years, this was largely confined to diagnostics. In the aforementioned case, since tissue samples from initial biopsy were insufficient to determine differentiation in the primary lesion, SSTR PET-CT played a critical role as a surrogate "whole body molecular biopsy", as coined by Chan and colleagues [11] and guided patient management by establishing eligibility for therapy, evaluating response, and providing long-term surveillance.

Theranostics expanded the role of the nuclear medicine physician beyond the reading room. Lu-177, with its high energy beta particles and medium energy gamma photons, allows imaging after therapy. Attaching it with a somatostatin analogue enables it to bind to somatostatin receptors in tumor cells directly exposing them to its cytotoxic beta radiation with a maximum particle range of 2 mm. The NETTER-1 trial established the efficacy of adding PRRT to the treatment of GEP NETs and other studies have since shown that PRRT can significantly improve overall survival and considerably decrease tumor burden [4,12,13]. Ultimately, PRRT has the benefit of dramatically improving quality of life [14]. In the patient, PRRT led to regression of the primary tumor and resolution of hepatic metastases, paving the way for definitive treatment in the form of surgery. A few studies have demonstrated the value of PRRT as neoadjuvant therapy, which facilitated resection in a few patients that were initially poor candidates for surgery [15,16,17]. To date, however, this is the first demonstration of the neoadjuvant application of PRRT in the local setting since its introduction to the Philippines in 2018 [7].

Finally, the multidisciplinary team plays an important role in optimizing the management of NETs. After close communication with the pathology service regarding the histopathologic and immunohistochemical findings, the medical oncologist then requested for the appropriate diagnostics and started the patient on somatostatin analogue therapy. Upon recognizing poor response, the medical oncologist then referred to the nuclear medicine theranostician for PRRT. The excellent response to PRRT then allowed the surgical team to successfully remove the tumor, which has since shown no evidence of recurrence after two years.

CONCLUSION

The case has shown that Ga-68 DOTATATE PET-CT can be a valuable tool in the different stages of management and that PRRT with Lu-177 DOTATATE can lead to a marked reduction of tumor burden. The effective use of these modalities radically changed the course of an initially inoperable patient and facilitated surgical resection of the residual tumor. In addition, multidisciplinary team engagement, as demonstrated in this case, can optimize the management of a metastatic well-differentiated pancreatic NET leading to a complete and sustained response with good quality of life for the patient.

ETHICAL CONSIDERATIONS

This report was conducted in adherence to the Principles of the Declaration of Helsinki and the Guidelines of the International Conference on Harmonization-Good Clinical Practice (ICH-GCP), and National Ethical Guidelines for Health and Health-Related Research [18,19].

ACKNOWLEDGEMENT

The authors would like to thank Dr. Rodelio D. Lim of the Institute of Pathology at St. Luke's Medical Center - Global City for providing the photomicrographs of the immunohistochemical stains.

REFERENCES

1. Langbein T, Weber WA, Eiber M. Future of Theranostics: An Outlook on Precision Oncology in Nuclear Medicine. J Nucl Med. 2019 Sep;60(Suppl 2):13S-19S. doi: 10.2967/jnumed.118.220566. PMID: 31481583.
2. Sgouros G, Bodei L, McDevitt MR, Nedrow JR. Radiopharmaceutical therapy in cancer: clinical advances and challenges. Nat Rev Drug Discov. 2020 Sep;19(9):589-608. doi: 10.1038/s41573-020-0073-9. Epub 2020 Jul 29. Erratum in: Nat Rev Drug Discov. 2020 Sep 7;: PMID: 32728208; PMCID: PMC7390460.
3. Starr JS, Sonbol MB, Hobday TJ, Sharma A, Kendi AT, Halfdanarson TR. Peptide Receptor Radionuclide Therapy for the Treatment of Pancreatic Neuroendocrine Tumors: Recent Insights. Onco Targets Ther. 2020 Apr 28;13:3545-3555. doi: 10.2147/OTT.S202867. PMID: 32431509; PMCID: PMC7205451.
4. Strosberg J, El-Haddad G, Wolin E, Hendifar A, Yao J, Chasen B, et al; NETTER-1 Trial Investigators. Phase 3 Trial of 177Lu-Dotatate for Midgut Neuroendocrine Tumors. N Engl J Med. 2017 Jan 12;376(2):125-135. doi: 10.1056/NEJMoa1607427. PMID: 28076709; PMCID: PMC5895095.
5. Hennrich U, Kopka K. Lutathera®: The First FDA- and EMA-Approved Radiopharmaceutical for Peptide Receptor Radionuclide Therapy. Pharmaceuticals (Basel). 2019 Jul 29;12(3):114. doi: 10.3390/ph12030114. PMID: 31362406; PMCID: PMC6789871.
6. National Comprehensive Cancer Network. NCCN Clinical Practice Guidelines in Oncology: Neuroendocrine and Adrenal Tumors (version 2.2022). 2022 Feb [cited 2023 January 12]. Available from: https://www.nccn.org/professionals/physician_gls/pdf/neuroendocrine.pdf.
7. Acayan EC, Bautista PA, Catangui MC, Cabatu-Key RR. The First Application of Ga-68 and Lu-177 Theranostics in the Philippines: A Rare Case of Mediastinal Small Cell Neuroendocrine Carcinoma. Philippine Journal of Nuclear Medicine, 2019, 14 (1), 5-8.
8. Bautista PA, Estrada MSJC and Fernando PEA. Almost complete response after a single peptide receptor radionuclide therapy as initial treatment for Merkel cell carcinoma with axillary lymph node metastases. World J Nucl Med 2019;18:324-44.
9. Perri G, Prakash LR, Katz MHG. Pancreatic neuroendocrine tumors. Curr Opin Gastroenterol. 2019 Sep;35(5):468-477. doi: 10.1097/MOG.0000000000000571. PMID: 31306159.
10. Ma ZY, Gong YF, Zhuang HK, Zhou ZX, Huang SZ, Zou YP, et al. Pancreatic neuroendocrine tumors: A review of serum biomarkers, staging, and management. World J Gastroenterol. 2020 May 21;26(19):2305-2322. doi: 10.3748/wjg.v26.i19.2305. PMID: 32476795; PMCID: PMC7243647.
11. Chan D, Bailey D, Schembri G, Bernard E, Hsiao E, Barnes T, et al. Dual 18F-fluorodeoxyglucose/68Gallium DOTATATE (FDG/DOTA) PET grading and histological grade in neuroendocrine tumours (NET). J Nucl Med [Internet]. 2016 May [cited 2023 January 12] 1;57(supplement 2):157 LP – 157. Available from: http://jnm.snmjournals.org/content/ 57/supplement_2/157.abstract
12. Brabander T, van der Zwan WA, Teunissen JJM, Kam BLR, Feelders RA, de Herder WW, et al. Long-Term Efficacy, Survival, and Safety of [177Lu-DOTA0,Tyr3]octreotate in Patients with Gastroenteropancreatic and Bronchial Neuroendocrine Tumors. Clin Cancer Res. 2017 Aug 15;23(16):4617-4624. doi: 10.1158/1078-0432.CCR-16-2743. Epub 2017 Apr 20. PMID: 28428192.
13. Das S, Al-Toubah T, El-Haddad G, Strosberg J. 177 Lu-DOTATATE for the treatment of gastroenteropancreatic neuroendocrine tumors. Expert Rev Gastroenterol Hepatol. 2019 Nov;13(11):1023-1031. doi: 10.1080/17474124.2019.1685381. Epub 2019 Oct 30. PMID: 31652074; PMCID: PMC7227421.
14. Maqsood MH, Tameez Ud Din A, Khan AH. Neuroendocrine Tumor Therapy with Lutetium-177: A Literature Review. Cureus. 2019 Jan 30;11(1):e3986. doi: 10.7759/cureus.3986. PMID: 30972265; PMCID: PMC6443107.
15. Sowa-Staszczak A, Pach D, Chrzan R, Trofimiuk M, Stefańska A, Tomaszuk M, et al. Peptide receptor radionuclide therapy as a potential tool for neoadjuvant therapy in patients with inoperable neuroendocrine tumours (NETs). Eur J Nucl Med Mol Imaging. 2011 Sep;38(9):1669-74. doi: 10.1007/s00259-011-1835-8. Epub 2011 May 11. PMID: 21559978; PMCID: PMC3151371.
16. Partelli S, Bertani E, Bartolomei M, Perali C, Muffatti F, Grana CM, et al. Peptide receptor radionuclide therapy as neoadjuvant therapy for resectable or potentially resectable pancreatic neuroendocrine neoplasms. Surgery. 2018 Apr;163(4):761-767. doi: 10.1016/j.surg.2017.11.007. Epub 2017 Dec 25. PMID: 29284590.

17. Opalińska M, Sowa-Staszczak A, Grochowska A, Olearska H, Hubalewska-Dydejczyk A. Value of Peptide Receptor Radionuclide Therapy as Neoadjuvant Treatment in the Management of Primary Inoperable Neuroendocrine Tumors. Front Oncol. 2021 Nov 12;11:687925. doi: 10.3389/fonc.2021.687925. PMID: 34868906; PMCID: PMC8633407.
18. World Medical Association. World Medical Association Declaration of Helsinki: ethical principles for medical research involving human subjects. JAMA, 2013, 310(20), 2191–2194. https://doi.org/10.1001/jama.2013. 281053.
19. Philippine Health Research Ethics Board. National Ethical Guidelines for Health and Health-related Research. DOST - PCHRD. 2017. [cited 2023 January 12] Available from: https://ethics.healthresearch.ph/index. php/2012-04-19-05-10-10/297-2017-nationalethical -guidelines-revision.

Adjunctive Role of Dual Time Point Imaging in Evaluating Bone Lesions with Increased ^{18}F-PSMA-1007 Uptake

Patrick Earl A. Fernando, MD, Jamilla Cecilia L. Gomez, MD

PET/CT Center, Cancer Institute, Chinese General Hospital and Medical Center, Manila, Philippines
E-mail address: patrixx.three@gmail.com

ABSTRACT

Background:

Non-specific focal uptake in the skeleton is a diagnostic pitfall on ^{18}F-PSMA-1007 PET/CT, but adjunctive measures to aid interpretation of these lesions are currently lacking. We present two cases where dual time point imaging provided additional information.

Case Presentation:

The first patient had a PI-RADS 3 lesion on MRI. No PSMA-avid abnormality was seen on PET, save for focal uptake in the right pubis with no anatomic correlate. Additional imaging showed a decrease in lesion SUV, and this was interpreted as benign. Another patient, diagnosed with prostate cancer, had multiple PSMA-avid pelvic foci. Two suspiciously malignant bone lesions had increasing SUV trend after dual time point imaging despite only faint sclerosis on CT. In contrast, one faint PSMA-avid lesion with no anatomic abnormality was read as benign after a decrease in SUV. A decrease in lesion SUV may point to a benign etiology, while an increase would heighten suspicion for malignancy. One possible molecular explanation is that a true PSMA-overexpressing lesion would bind to the tracer for a longer period than a false positive.

Conclusion:

Dual time point imaging provides additional information that may be useful in the interpretation of non-specific skeletal lesions with increased ^{18}F-PSMA-1007 uptake.

Keywords: *^{18}F-PSMA-1007 PET/CT, bone lesions, dual time point imaging*

INTRODUCTION

Prostate-specific membrane antigen (PSMA) has become a gamechanger in nuclear medicine when it comes to prostate cancer imaging and therapy. Specifically, PSMA positron emission tomography/computed tomography (PET/CT) has become the modality of choice for staging and evaluating biochemical recurrence. When locally available, it is also used to assess eligibility for PSMA radioligand therapy.

Over the past decade, a number of PSMA PET radiopharmaceuticals have been produced for commercial use. In our local setting, ^{18}F-PSMA-1007 and ^{68}Ga-PSMA-11 are available. ^{18}F-PSMA-1007 has a longer half-life than its Ga-68 counterpart, thereby allowing for centralized mass production. Its primary mode of excretion is through the hepatobiliary tree; hence, instances where urinary bladder activity obscures the prostate gland are reduced [1]. Also, ^{18}F-PSMA-1007 PET/CT is locally offered at a lower price point than ^{68}Ga-PSMA-11 PET/CT, which is important in places where PET/CT scans are not reimbursed by the national health insurance service.

One potential disadvantage of ^{18}F-PSMA-1007 PET/CT is the higher reported incidence of PSMA-avid non-specific bone lesions (NSBLs). Otherwise known as unspecific bone uptake (UBU), these are skeletal foci of increased PSMA uptake which are equivocal for metastatic bone disease [1, 2]. A matched-pair comparison showed almost 5 times as many PSMA-avid benign bone lesions in ^{18}F-PSMA-1007 PET scans relative to ^{68}Ga-PSMA-11 PET scans [3]. This is supported experientially by the authors, who attest to seeing NSBLs mentioned more frequently in ^{18}F-PSMA-1007 PET reports than in their

^{68}Ga-PSMA counterparts. While these lesions typically do not have morphologic correlates, beginning bone metastasis may present as such. This may lead to either overstaging (interpreting a NSBL as metastatic when it is not) or understaging (calling a truly metastatic NSBL as inflammatory) and may have serious consequences on patient management.

The challenge of interpreting these NSBLs is not lost to those who interpret ^{18}F-PSMA-1007 PET/CT images on a regular basis. Vollnberg et al. retrospectively analyzed biopsy results of 11 NSBLs from 10 patients, of which only one revealed true metastasis. On review of imaging, 8 of the 11 foci were classified as high-risk for malignancy, and none of these lesions had corresponding CT abnormalities [4]. Arnfield et al. suggests the use of cut-offs on standard uptake values (SUVs). Lesions with a maximum SUV (SUVmax) less than 7.2 are likely benign, while those with SUVmax between 7.2 and 11.1 may be equivocal or metastatic, depending on clinical risk factors, scan appearance, and patient management implications [1].

In our center, dual time point (or delayed) imaging is a common method used to acquire further information on equivocal-looking foci of increased tracer uptake. When deemed necessary, a repeat scan of a section of the patient's body is obtained, usually post-void imaging of the pelvis. It is more commonly employed in ^{18}F-fluorodeoxyglucose (FDG) and ^{68}Ga-PSMA-11 PET scans where radioactivity from other organs, commonly in the gastrointestinal tract, may preclude proper evaluation of significant-looking lesions. In a study by Aksu et al., dual time-point imaging with ^{68}Ga-PSMA-11 PET was shown to aid in differentiating Gleason grade groups [5]. In the context of ^{18}F-PSMA-1007 PET scans, this technique is usually applied in patients with apparently impaired hepatobiliary excretion where urinary activity may obscure the prostate. This incidentally allows further elucidation of NSBLs in pelvic bones based on appearance and SUV change between the two time points.

We present two cases where dual time point imaging aided in the interpretation of NSBLs on ^{18}F-PSMA-1007 PSMA PET/CT. All SUVs reported are SUVmax unless otherwise specified.

CASE 1

A 76-year-old came to our center with history of lower urinary tract symptoms and benign prostate biopsy findings from three years ago. Surveillance studies from two months prior showed prostatomegaly with a PI-RADS 3 lesion in the left posterolateral to posteromedial peripheral zone and a serum prostate-specific antigen (PSA) value within normal limits at 3.18 ng/mL. PSMA PET/CT imaging was requested by the urologist for further evaluation of possible malignancy. Initial whole-body PET images were acquired 63 minutes after PSMA administration, with delayed imaging of the pelvis done at 84 minutes post-injection.

The PET scan showed diffusely increased PSMA uptake in an enlarged prostate gland (SUV 6.9, Figure 1A). No PSMA abnormality corresponding to the MRI finding was seen. Additionally, a PSMA-avid focus was noted in the right pubic bone (Figure 1B), with no correlate on both diagnostic CT and the prior MRI. Emission images of the pelvis acquired 21 minutes after initial whole-body imaging showed a decrease in lesion SUV from 6.6 to 5.8. Taken together, the findings were signed out as favoring benign prostatic hypertrophy, with the bone lesion being more likely inflammatory or non-specific. Continued monitoring, both biochemically (serum PSA) and through imaging, was advised.

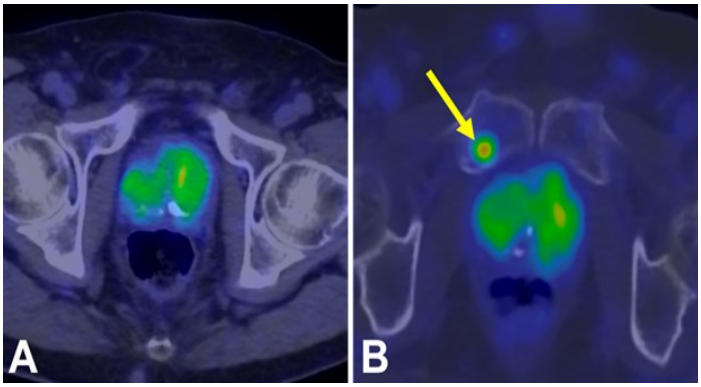

FIGURE 1. PSMA PET/CT images of a 76-year-old patient with a suspicious prostate MRI finding. Apart from diffuse PSMA uptake in the prostate (A), a PSMA -positive right pubic bone lesion was also noted (B), which decreased in SUV after delayed imaging

CASE 2

A 68-year-old with elevated PSA (21.93 ng/mL) and biopsy-proven prostate adenocarcinoma (Gleason score 4+3) was referred to our center. MRI one month prior showed multifocal PI-RADS 4-5 prostatic disease and a suspicious enhancing lesion involving the left superior pubic ramus. PSMA PET/CT was subsequently requested for metastatic work-up. Initial whole-body PET images were acquired 70 minutes after PSMA administration, with delayed imaging of the pelvis done at 103 minutes post-injection.

Apart from multiple PSMA-avid foci in the prostate which coincided with findings in the prior MRI, several pelvic bone lesions with increased PSMA uptake were also seen. These are summarized in Table 1, along with their SUVs on initial and additional emission imaging (done 33 minutes after initial acquisition). The left pubic and left iliac wing lesions with increasing SUV were suspected as beginning bone metastasis, while the faint PSMA-avid lesion near the sacroiliac joint was interpreted as likely degenerative.

DISCUSSION

A PubMed advanced search using the syntax "PSMA-1007 AND bone" would yield 305 publications at the time of this writing. However, after manually filtering the results, less than 10 actually discussed NSBLs. It can thus be said that based on the current body of knowledge on this topic, there is more than ample room for further research.

TABLE 1. PSMA-avid pelvic bone lesions in the PSMA PET/CT of a 68-year-old with prostate carcinoma. PET images were windowed to the same scale to allow visual comparison.

Lesion location	Left superior pubic ramus	Left iliac wing, lateral aspect	Left iliac wing, proximal to
MRI correlate	Enhancing lesion (Figure 2)	None	None
CT correlate	Very faint sclerosis	Faint sclerosis	None
SUV, initial	4.0	6.1	3.8
SUV, delayed	6.5	6.5	2.9
Lesion image	Figure 3A	Figure 3B	Figure 3C

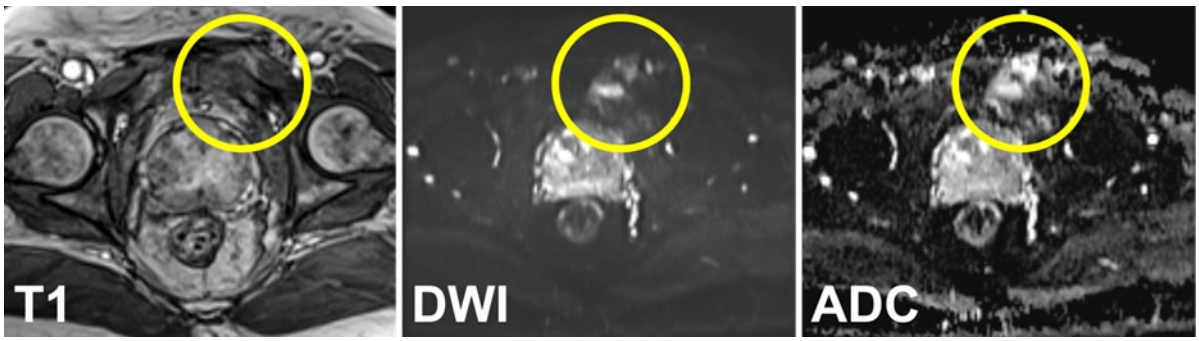

FIGURE 2. MRI showed an abnormality in the left superior pubic ramus.

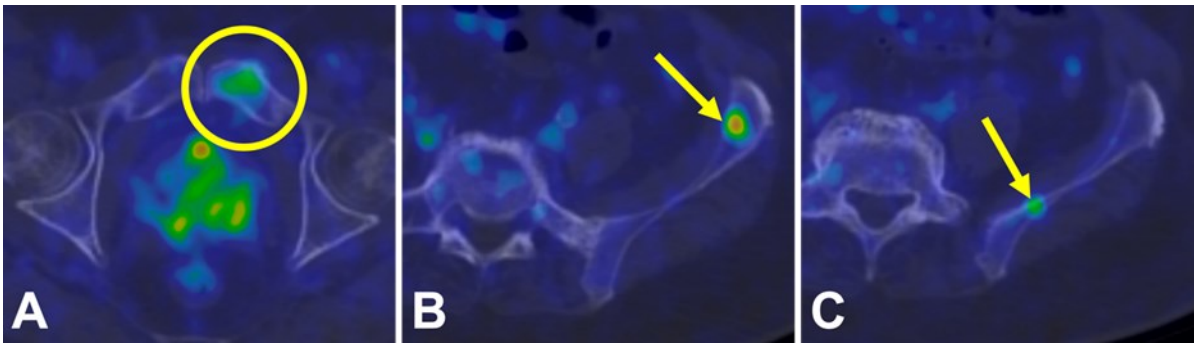

FIGURE 3. PSMA PET/CT images of the three PSMA-avid pelvic bone lesions, as described in Table 1

To the knowledge of the authors, this is the first attempt to provide a possible imaging approach in the evaluation of equivocal bone lesions on ^{18}F-PSMA-1007 PET/CT scans. The two cases both involve pelvic bone lesions and have dual time point images, but their clinical backgrounds and indications for imaging are different.

The first patient had no known malignancy. The clinician was ruling out malignancy given a PI-RADS 3 lesion on a prior MRI, hence PSMA PET/CT evaluation was requested. The MRI lesion had no PET correlate but diffuse prostatic PSMA avidity was seen. Using the recently published PRIMARY scoring system for patients clinically suspected with prostate cancer, this lesion would have a score of 1, thus decreasing the probability of metastasis should other PSMA-avid findings be encountered [6]. Additionally, a PSMA-avid bone focus was seen in the right pubis. The tracer washout manifested by an SUV decrease on dual time point imaging, on top of the lack of a distinct CT correlate, supports a benign interpretation of this finding.

In contrast, the second patient was already diagnosed with prostate cancer, and PSMA PET/CT was performed for staging. Two PSMA-avid bony foci had faint sclerosis on CT, with one of them also having an MRI correlate. In both cases, an increase in SUV was noted on dual time point imaging, which increased reader confidence in interpreting these lesions as beginning metastasis. A third lesion was seen which was fainter than the previous two, had no CT correlate, and showed a decreasing SUV trend. Based on this, as well as its proximity to the sacroiliac joint, the lesion was interpreted as degenerative.

All the mentioned bone lesions in both cases had SUVmax values below the previously described threshold of 7.2 [1]. Using this cut-off without anatomic correlates, some of the abovementioned skeletal foci would have been labeled as benign. SUV change on dual time point imaging thus provides additional information in discriminating between possibly benign and possibly malignant bone lesions. A molecular-level explanation for this phenomenon still needs to be elucidated. However, it can be postulated that true PSMA-overexpressing lesions would have more favorable receptor binding kinetics toward the tracer compared to false positives where tracer washout is seen. Bone lesion biopsy remains to be the best means of confirming such hypothesis, but financial and ethical hurdles in the local setting are dissuasive for independent research.

This case report highlights the potential adjunctive value of dual time point imaging in the interpretation of NSBLs with increased ^{18}F-PSMA-1007 UBU. Further studies are recommended to establish the utility of dual time point imaging under such context on a larger scale. This includes prospective follow-up to confirm the benign or malignant nature of the bone lesions, as well as possible integration in future imaging protocols and guidelines, such as the optimal interval time of second scan imaging.

REFERENCES

1. Arnfield EG, Thomas PA, Roberts MJ, Pelecanos AM, Ramsay SC, Lin CY, et al. Clinical insignificance of [^{18}F] PSMA-1007 avid non-specific bone lesions: a retrospective evaluation. Eur J Nucl Med Mol Imaging. 2021;48:4495-4507. doi: 10.1007/s00259-021-05456-3. PMID: 34136957.
2. Grünig H, Maurer A, Thali Y, Kovacs Z, Strobel K, Burger I, et al. Focal unspecific bone uptake on [^{18F}]-PSMA-1007 PET: a multicenter retrospective evaluation of the distribution, frequency, and quantitative parameters of a potential pitfall in prostate cancer imaging. Eur J Nucl Med Mol Imaging. 2021;48:4483-4494. doi: 10.1007/s00259-021-05424-x. PMID: 34120201. PMCID: PMC8566387.
3. Rauscher I, Krönke M, Konig M, Gafita A, Maurer T, Horn T, et al. Matched-pair comparison of ^{68}Ga-PSMA-11 PET/CT and ^{18}F-PSMA-1007 PET/CT: frequency of pitfalls and detection efficacy in biochemical recurrence after radical prostatectomy. J Nucl Med. 2020;61(1):51-57. doi: 10.2967/jnumed.119.229187. PMID: 31253741. PMCID: PMC6954457.
4. Vollnberg B, Alberts I, Genitsch V, Rominger A, Afshar-Oromieh A. Assessment of malignancy and PSMA expression of uncertain bone foci in [^{18}F]PSMA-1007 PET/CT for prostate cancer – a single-centre experience of PET-guided biopsies. Eur J Nucl Med Mol Imaging. 2022 Apr 28. doi: 10.1007/s00259-022-05745-5. PMID: 35482114. PMCID: PMC9399054.
5. Aksu A, Topuz Ö, Yilmaz G, Çapa Kaya G, and Yilmaz B. Dual time point imaging of staging PSMA PET/CT quantification; spread and radiomic analyses. Ann Nucl Med. 2022;36(3):310-318. doi: 10.1007/s12149-021-01705-5. PMID: 34988888.
6. Emmett L, Papa N, Buteau J, Ho B, Liu V, Roberts M, et al. The PRIMARY score: using intraprostatic 68Ga-PSMA PET/CT patterns to optimize prostate cancer diagnosis. J Nucl Med. 2022;63(11):1644-1650. doi: 10.2967/jnumed.121.263448. PMID: 35301240. PMCID: PMC9635676.

transmedic

LEADING MEDICAL EQUIPMENT SPECIALIST IN SOUTHEAST ASIA

ABOUT US •••

TRANSMEDIC PHILIPPINES, INC. currently serves the needs of some of the country's top hospitals and medical clinics for - *external beam radiation therapy and also radiation therapy planning system, radiofrequency ablation systems & clinical support, vascular imaging requirements, LDR brachytherapy requirements, laparoscopy towers, beds, and other advanced medical technologies.* All in all, the Company has stood for the introduction of new technology for use in the local medical market to improve patient care & services, and/or to optimize cost efficiency.

LEARN MORE •••

+632 53176888
info.ph@transmedicgroup.com
http://www.transmedicgroup.com/

ANSTO
Science. Ingenuity. Sustainability.

SPECTRUM DYNAMICS MEDICAL

DDD Diagnostic

oasis

mim Encore

mim Assistant

Best ABT Molecular Imaging

mim SOFTWARE

UNITED IMAGING

mim SurePlan MRT

Eckert & Ziegler

SurePlan LiverY90

MERCK

Levothyroxine sodium

Euthyrox® 25 mcg, 100 mcg
50 mcg, 150 mcg

Mitigating the Dilemma in Dementia: A Case Series of the First Amyloid Brain PET scans in the Philippines

Lara Triccia C. Luistro, MD[1] , Eduardo Erasto S. Ongkeko, MD,[1,2]

[1]*Department of Nuclear Medicine and Theranostics, St. Luke's Medical Center, Global City*
[2]*Department of Nuclear Medicine and Theranostics, St. Luke's Medical Center, Quezon City*
E-mail address: ltcluistro@stlukes.com.ph

ABSTRACT

Diagnosis of Alzheimer dementia is done clinically using criteria set by different neurological associations. Inevitably, clinicians encounter cases that do not fulfill the set definitions and have to resort to supporting data to form a clinical judgment. Part of the ancillary work-up for dementia is the brain amyloid PET scan that has recently been available in the Philippines. It involves a radiopharmaceutical with high-affinity binding to amyloid plaques which for a time were thought to be central pathological finding for Alzheimer dementia. This study describes the first four amyloid PET scans in the Philippines and detail the protocol as well as interpretation of such studies. The procedure is not as simple and reproducible as one might think hence following the recommended protocol and interpretation guidelines are of utmost importance. We recommend standardization of the reporting of results for all centers that will cater to patients being worked up for dementia, which include reporting SUVRs for both whole cerebellum and cerebellar cortex. More studies are recommended to generate a local Florbetaben SUVR cutoff.

.

***Keywords**: amyloid PET, Alzheimer disease, diagnostic imaging, F-18 Florbetaben*

INTRODUCTION

Alzheimer's Disease

Alzheimer's disease (AD) is the most common cause of dementia accounting for two-thirds of cases. The World Alzheimer Report 2015 has estimated that 46.8 million people worldwide are living with dementia [1]. Dominguez et al. has projected the Philippines to have a total of 1,474,588 dementia cases in 2030, 1,972,067 in 2040 and 2,529,436 in 2050 with incidence at 16 per 1,000 person-year [2]. AD is a disease of the elderly, most commonly presenting at the age of 65, which presents insidiously with progressive decline. It is characterized by an accumulation of abnormal neuritic plaques and neurofibrillary tangles. Definitive diagnosis of AD requires histopathologic evidence of plaques and tangles demonstrated by Alois Alzheimer himself. The widely adapted clinical criteria used is by the National Institute on Aging and the Alzheimer's Association (NIA-AA) updated in 2011 and the Diagnostic and Statistical Manual of Mental Disorders (DSM) criteria revised in 2013. However, diagnosis is still confounded by atypical presentations such as early age and rapid decline thus the need to combine clinical features with imaging and cerebrospinal fluid (CSF) biomarkers. The National Institute on Aging-Alzheimer's Association (NIA-AA) workgroups also set criteria to help differentiate neurocognitive (NCD) subtypes using two classes of biomarkers to help diagnose AD, namely biomarkers for brain amyloid Aβ protein deposition detection and the biomarkers for downstream neuronal injury identification [3]. Evidence of amyloid deposition is based on reduced cerebrospinal fluid (CSF) Aβ42 levels and positive PET amyloid imaging, whereas the latter includes three major biomarkers, namely elevated CSF tau, reduced fluorine-18 fluorodeoxyglucose (F-18 FDG) uptake on PET in the temporoparietal lobes, and disproportionate atrophy at the medial, basal, and lateral temporal lobes on structural MRI scans. There is also a proposed staging of preclinical AD which involves objective evidence of amyloidosis with and without neurodegeneration and subtle cognitive decline.

Anatomical imaging modalities show cortical atrophy from neuronal degeneration and eventual cell loss. Different patterns of loss are associated with disease. Many, if not most, clinicians would request for the widely available MRI to support diagnosis of AD as well as to exclude other organic pathologies that can cause cognitive impairment. MRI findings of AD include widening of ventricles, parietal sulcal widening and atrophy of the posterior cingulate gyrus and precuneus, hippocampus and parahippocampal gyrus [4]. Several

scoring systems have been used as guides to assess NCD such as medial temporal lobe atrophy score, posterior cortical score and global cortical atrophy scale. The GCA scale evaluates 13 brain regions and may be confounded by age. Medial temporal atrophy is associated with mild cognitive impairment (MCI) and AD and the medial temporal lobe atrophy (MTA) score is less affected by normal aging. Posterior cortical atropy on the other hand is associated with early-onset AD and is helpful for the evaluation of atypical AD.

Positron Emission Tomography (PET)

PET becomes a marker of neuronal injury as damaged brain cells exhibit decreased uptake of F-18 FDG [5,6] and as a marker of amyloid plaque deposition when the cortex demonstrates increased uptake of the amyloid tracers. F18-FDG brain PET shows hypometabolism even before overt atrophy occurs, reflecting not only loss of cells but impaired synaptic transmission. Patterns of disease-specific decreased tracer uptake allowed F-18 FDG PET to be assist in the diagnosis of different NCDs and as prognosticating factor to predict which patients who have MCI can progress to Alzheimer dementia with reported 75-100% accuracy [7]. Advances in brain PET imaging include development of radiotracers that bind to amyloid plaques themselves. The first one to be developed is C11- Pittsburgh compound B followed by Fluorine18-based tracers like Florbetaben, Flutemetamol and Florbetapir. C11- Pittsburgh compound B use is limited to facilities who have cyclotron on-site owing to its short 20-minute half-life. Subsequent US FDA-approved F-18 radiopharmaceuticals are now preferentially used because of their longer 109.8 minute half-life. These amyloid tracers bind non-specifically to white matter and have no uptake in normal gray matter. Amyloid brain PET scans are semi-quantified into positive and negative. Negative scans demonstrate binding only the cerebral white matter while a positive scan shows uptake in both gray and white matter and hence shows loss of contrast between the two. Amyloid deposition starts even before the onset of cognitive impairment and can be seen in both AD patients and elderly patients with normal cognition hence its strength lies in its high negative predictive value, with a negative scan giving a very low likelihood of AD.

The Amyloid Imaging Task Force (AIT) was developed by the Society of Nuclear Medicine and Molecular Imaging (SNMMI) and Alzheimer's Association to determine the Appropriate Use Criteria (AUC) of amyloid brain PET imaging [8]. The AUC will assist clinicians to determine the potential value doing an amyloid PET scan can add. It is still important to emphasize that a positive scan is not tantamount to a clinical diagnosis of Alzheimer's and that it is the ultimate clinical judgment of the clinician to decide on the diagnosis. The AIT established the following as the preamble, or the common characteristics, for patients whom AUC may be applied: presence of cognitive impairment, possibility of AD as a diagnosis and evidence of the amyloid positivity to increase diagnostic certainty, ideally sufficient to shift the management. Three appropriate indications were concluded which include 1) patients with progressive and persistent unexplained mild cognitive impairment 2) patients with possible AD (atypical course and with concomitant organic disease) and 3) progressive dementia and atypical age of onset. For the first indication, an amyloid-negative scan on the background of MCI will lead towards investigation of other causes of impairment such as vascular or traumatic. Also, combining amyloid positivity with unexplained MCI will increase the level of certainty that early AD is the cause and that it should subsequently follow that a change in management is warranted. For the second indication, it is mainly to exclude patients with typical AD and to further investigate patients already diagnosed with dementia presenting atypically or if the course is difficult to assess and those with other concomitant pathology. Lastly, amyloid PET scan may be used for patients who are young but already presenting with dementia to help plan an early course of management. Amyloid PET scan has been recommended against patients who satisfy the core-clinical criteria of AD, to determine dementia severity, to diagnose disease in those with genetic predisposition as well as determine genetic mutations, those who have cognitive complaints not confirmed clinically, asymptomatic patients and those for non-medical purposes.

Imaging Acquisition and Interpretation from SNMMI

Based on the SNMMI recommendations, physicians who interpret amyloid PET scans should have specialized in Nuclear Medicine and completed appropriate training programs from the manufacturer. Likewise, amyloid PET scans should be performed by qualified Nuclear Medicine Technologists certified by the appropriate board.

The study requisition should include 1) appropriate clinical information about the patient to justify the study

and to allow appropriate exam/study coding; 2) information about the ability of the patient to cooperate for the test is helpful; and 3) information about current medications in case mild sedation is necessary. It is also helpful to know if the patient needs to be accompanied by a guardian.

Protocol/Image acquisition

1. Before scanning, the patient should empty their bladder for maximum comfort during the study.
2. The patient should be supine with suitable head support. The entire brain should be in the field of view, including the entire cerebellum. Avoid extreme neck extension or flexion if possible. To reduce the potential for head movement, the patient should be as comfortable as possible with the head secured as completely as possible. Tape or other flexible head restraints may be employed and are often helpful.
3. ^{18}F-florbetapir, ^{18}F-flutemetamol and ^{18}F-florbetaben should be injected as a single intravenous slow-bolus in a total volume of 10 ml or less. The dose/catheter should be flushed with at least 5-15 ml 0.9% sterile sodium chloride to ensure full delivery of the dose.
4. The recommended dose/activity, waiting period, and image acquisition duration are summarized in Table 1.
5. Image acquisition should be performed in 3D data acquisition mode with appropriate data corrections.
6. Image reconstruction should include attenuation correction with typical transaxial pixel sizes between 2-3 mm and slice thickness between 2-4 mm.
7. Advise the patient to hydrate and void after the scanning session to diminish radiation exposure.

Amyloid PET imaging is interpreted both qualitatively and quantitatively. Qualitative examination by PET readers is through visual inspection of tracer deposition in the cortical gray matter of areas commonly affected in Alzheimer disease. These may be categorized into brain amyloid plaque load (BAPL) 1, 2 and 3 for no significant amyloid deposition, minor deposition, and significant deposition, respectively. BAPL 1 is amyloid-negative while BAPL 2 and 3 are positive.

OBJECTIVES

General Objective

To describe the first four Amyloid PET scans in the country, its procedure, and findings

Specific Objectives

To describe the profile of patients who underwent Amyloid PET (age, gender, indication for the scan)
To discuss the appropriate use criteria for requesting Amyloid PET

METHODS

This is a retrospective case series of four patients who underwent Amyloid brain PET scans at St Luke's Medical Center - Quezon City and Global City from July to August 2022.

Criteria for Subject Selection

Inclusion Criteria

The first four patients who completed a brain PET scan using an amyloid tracer

Exclusion Criteria

- Significant neurological disease other than early Alzheimer's disease.
- Major psychiatric disorder or symptom that can explain patient's condition
- Unstable medical conditions

Operational definitions

Brain amyloid PET scan or amyloid brain PET scan - PET scan specific for evaluating the brain using F-18 florbetaben, a radiotracer which is avid to the amyloid plaques implicated in Alzheimer's disease.

TABLE 1. Recommended Dose/Activity, waiting period and image acquisition

Radiotracer Recommended	Dose /Activity	Waiting Period	Acquisition
^{18}F-florbetapir	370 MBq (10 mCi)	30-50 minutes	10 minutes
^{18}F-flutemetamol	185 MBq (5 mCi)	90 minutes	10-20 minutes
^{18}F-florbetaben	300 MBq (8 mCi)	45-130 minutes	20 minutes

Positron emission tomography scan (PET) scan - a nuclear medicine imaging procedure using a positron-emitting nuclide to image desired parts of the body. Tracers used are dependent on the lesion being evaluated

Standardized uptake value (SUV) – a semiquantitative measurement of radiopharmaceutical uptake of a region of interest normalized to dose/radioactivity administered and volume of distribution in the body (weight or lean body mass).

SUV maximum (SUVmax) – highest SUV value in a given lesion or region of interest.

SUV mean (or mean SUV)– average SUV counts in the whole region of interest.

SUV ratio (SUVR or SUVratio) – for brain amyloid PET scans, this is the ratio of the mean SUV of the region of interest divided by the mean SUV of the reference brain region.

Description of Study Procedure

The researchers will review the database, scans, and results of the four patients who underwent Amyloid PET scans at St. Luke's Medical Center. The information will include:

- Age
- Sex
- Neurologic manifestations reported at the time of the scan
- Comorbidities
- Other imaging modalities
- Prior treatment done if any

Sample Size Estimation

No sample size was computed because only the first two patients from each branch of the hospital are included.

Data Analysis

Descriptive statistics were used to summarize the demographic and clinical characteristics of the patients.

Radiopharmaceutical

Neuraceq (F-18 Florbetaben) is the locally available radiotracer for amyloid. It comes in a clear vial of 300 MBq/mL colorless solution. Similar to Fluorine-18 - based radiotracers, it decays with a half-life of approximately 110 minutes by emitting a positron radiation of 634 keV, followed by photonic annihilation radiation of 511 keV. The solution contains 30 mg sodium and 15vol% of ethanol.

The manufacturer recommends use with no dose adjustment based on age and weight. Other precautions are similar to the other radiopharmaceuticals. The medication is administered slowly via intravenous route followed by flushing using normal saline solution. For our institution, the F18-Florbetaben radiopharmaceutical is delivered by a third-party supplier.

Amyloid PET scan protocol

The following protocol is derived from the Amyloid Brain PET/CT protocol of St. Luke's Medical Center - Global City and Quezon City

- Verify patient identification (Name and date of birth at the very least)
- Verify doctor's request: (PET tracer properly indicated , with or without diagnostic CT)
- Bring patient to PET lounge and measure height and weight
- Take patient's clinical history
- Explain procedure, possible side effects and radiation precautions
- Secure consent for the procedure
- Insert IV line (or secure permission for central line access)
- Preparation of dose (re-check label of vial delivered)
- Dispense 8mCi (300 MBq) into a syringe and place in a lead-shielded container
- Recheck patency of IV line and administer radiopharmaceutical to the patient via slow IV push followed by a 10mL- saline flush
- Measure post-injection activity from the syringe and record time of administration
- Ask patient to void prior to scanning
- Perform PET scan, with or without diagnostic CT and with or without sedation, 90 minutes after tracer administration
- Strap and secure the patient to the scanning table and provide adequate head support to minimize patient motion
- Adjusts the height of the scanner table to its isocenter at 185.
- Starts the Dual CT surview (AP and Lateral Views). When the CT surview is complete, the surview image displays with a plan series box.

- Move and adjust the plan scan box for PET acquisition from base of the skull to about 1 inch above the tip of the cranium. The scan plan box for Low-dose CT will automatically adjust to the same region of interest as that of PET acquisition.
- Perform the scan of 1 bed with 20 minutes acquisition
- Nuclear Medicine physician checks scan
- Escort the patient back to the lounge and patient is sent home

PET Amyloid Interpretation

Once acquired, emission PET images and low-dose CT are sent to workstations for interpretation. Both branches of the hospitals use Biograph Vision PET/CT scanner and syngo.via workstations (Siemens Healthineers) for interpreting amyloid PET scans. These scans are read using the MM Neurology software by Siemens. The software is capable of processing images acquired using the three F-18 - based tracers against the CT attenuation correction map generated prior to the PET emission images. Non-attenuation correction images may also be used. Other imaging modalities the patients had prior were not used for correction. Options also for normalizing images using cerebellar and whole brain images are available as well. Once the images are processed, nuclear medicine physicians may view them in the axial, sagittal and coronal slices together with maximum-intensity projections. Software-generated ROIs for the cerebral and cerebellar lobes, anterior and posterior cingulate gyri, basal ganglia, and ventricles are also provided but ultimately determined by the reader. Physicians then proceed to determine F-18 Florbetaben localization. The readers compare the cortical gray matter signal intensity to the maximum white matter signal intensity. The images should be viewed in a systematic manner starting at the level of cerebellum and scrolling up through the lateral temporal and frontal lobes, then to the area of the posterior cingulate cortex and precuneus, and finally to the parietal lobe.

The manufacturers recommend scoring each reference brain region (lateral temporal lobes, frontal and parietal lobes, and precuneus/posterior cingulate gyri) as to no tracer uptake (1), moderate trader uptake (2) and pronounced tracer uptake (3), known as the regional cortical tracer uptake (RCTU) score. Brain amyloid plaque load (BAPL) scores are subsequently derived from the RCTU. BAPL 1 corresponds to having an RCTU score of 1 in each of the four brain regions (lateral temporal lobes, frontal lobes, posterior cingulate/precuneus, parietal lobes), while BAPL 2 corresponds to RCTU 2 in any or all of the four brain regions and no score of 3 in any. BAPL 3 is an RCTU score of 3 at least in one of four brain regions. BAPL 1 is the amyloid-negative scan while BAPL scores 2 and 3 are considered positive scans.

SUVRs are then computed manually by comparing the uptake values of the cortical ROI versus the cerebellar cortex with or without the whole cerebellum.

Results

Three of the four patients were elderly and one of which was in the late middle-age. Three were male. Two of the patients had stable comorbidities.

Mean radioactivity at the time of injection was 294.7 MBq of F-18 Florbetaben. Imaging was performed using a Siemens Biograph Vision 64 slice PET/CT scanner and acquired with a mean time of 90.7 minutes post tracer injection.

No reported adverse reactions to the radiotracer were noted in the four patients.

Case 1

The first patient is a 73-year-old female, hypertensive, dyslipidemic and presents with cognitive impairment. She has memory loss of recent events and with immediate recall (inability to recall details of instructions, repetitive), fears getting lost, needs assistance with maintenance medications, has word finding difficulty, not oriented to time but oriented to place, unable to construct simple geometric figures and clock drawing test. Patient is able to perform some activities of daily living and needs assistance in some. She has already been diagnosed clinically as a case of Alzheimer dementia and was previously treated with acetylcholinesterase inhibitors. Patient underwent PET amyloid imaging as a volunteer case for St. Luke's Quezon City.

Brain MRI done one year prior showed mild atrophy in the frontal, temporal and parietal lobes with mild atrophy of the choroid fissure while cognitive testing atrophy of the choroid fissure while cognitive testing reported mild Alzheimer dementia. At the time of the scan, the patient's symptoms were essentially stable.

Patient underwent the PET scan at 93 minutes post tracer injection and because of patient movement, nuclear medicine physicians decided on a delayed scan 123 minutes post tracer injection. Results showed loss of gray-white matter differentiation in the frontal lobes, parietal lobes, posterior cingulate gyrus, and lateral temporal lobes. Brain amyloid plaque load (BAPL) evaluation shows moderate beta-amyloid deposition in the aforementioned regions. SUVRs were all above the 1.478 cut-off set by Sabri et al. in 2015 including the anterior cingulate gyrus and occipital lobes [9]. The observed increase in the SUVrs during the subsequent scan however did not provide additional information other than quality control since all mean SUVs of reference regions have declined.

Quantitative analysis using the standard uptake value ratios (SUVR) normalized to the cerebellar cortex are as shown in Table 2.

Case 2

The second patient is a 56-year-old female who presented with short-term memory loss at 54 years old and family history of Alzheimer's disease. She was started on an acetylcholinesterase inhibitor one month prior to the brain PET scan. She had hysterectomy and unilateral ovarian surgery for benign findings and had no other comorbidities. A PET Amyloid scan was requested to increase diagnostic probability of early onset dementia.

Visually, there is loss of gray-white matter differentiation in the anterior and posterior cingulate gyri, frontal, parietal, occipital, and temporal lobes with corresponding elevated SUVRs as shown in Figure 2 and Table 3.

Case 3

The third patient is an 82-year-old female who complains of delayed recall and derangement in fluency. Prior brain MRI in October 2018 reported a chronic infarct in the left frontal region without any residuals. However no recent imaging modality was acquired. Patient had no prior treatment. Patient has no known comorbidities.

PET amyloid imaging acquired 90 minutes after tracer injection showed Florbetaben distribution in the white matter of the cerebrum and cerebellar peduncles. No undue florbetaben uptake is seen in the cerebral cortical gray matter. There is no loss of florbetaben gray/white matter contrast. SUVRs normalized to the cerebellar cortex were below 1.478 (see Figure 3 and Table 4).

Diagnostic CT done together with the PET scan showed no evidence of acute territorial infarct, intracranial hemorrhage or focal mass lesion with probable chronic small vessel ischemic changes, gliosis, and/or demyelination. There was mild symmetric widening of the cerebral cortical sulci on both sides, both Sylvian fissures and basal cisterns as well as the cerebellar interfolial spaces relating to volume loss. The ventricles are normal in size and configuration.

Case 4

The fourth patient is a 74-year-old male presenting with recent and distant memory loss. Recent brain MRI reported cerebral atrophy that was not uncommon for patient's age. She has no known comorbidities and no prior treatment.

PET scan acquired 90 minutes post tracer injection showed good contrast between white and gray matter in all the reference regions (see Figure 4 and Table 5).

Discussion

The AIT aimed to address several questions with regards to the application of the amyloid PET scan namely proof of technical efficacy, diagnostic accuracy, and clinical utility.

Proof of technical efficacy includes reproducibility of specific amyloid PET acquisition procedures and protocols under standardized conditions and must be applicable to the range of PET instrumentation in use.

Tracer preparation, including quality control from the third-party supplier is monitored by the manufacturer of the tracer itself. As needed site visits are conducted should concerns arise from generating the tracer. St. Luke's Medical Center makes use of the protocol as recommended in the 2016 Society of Nuclear Medicine and Molecular Imaging Procedure Standard – European Association of Nuclear Medicine Practice Guideline for Amyloid PET Imaging of the Brain. Prior to conducting

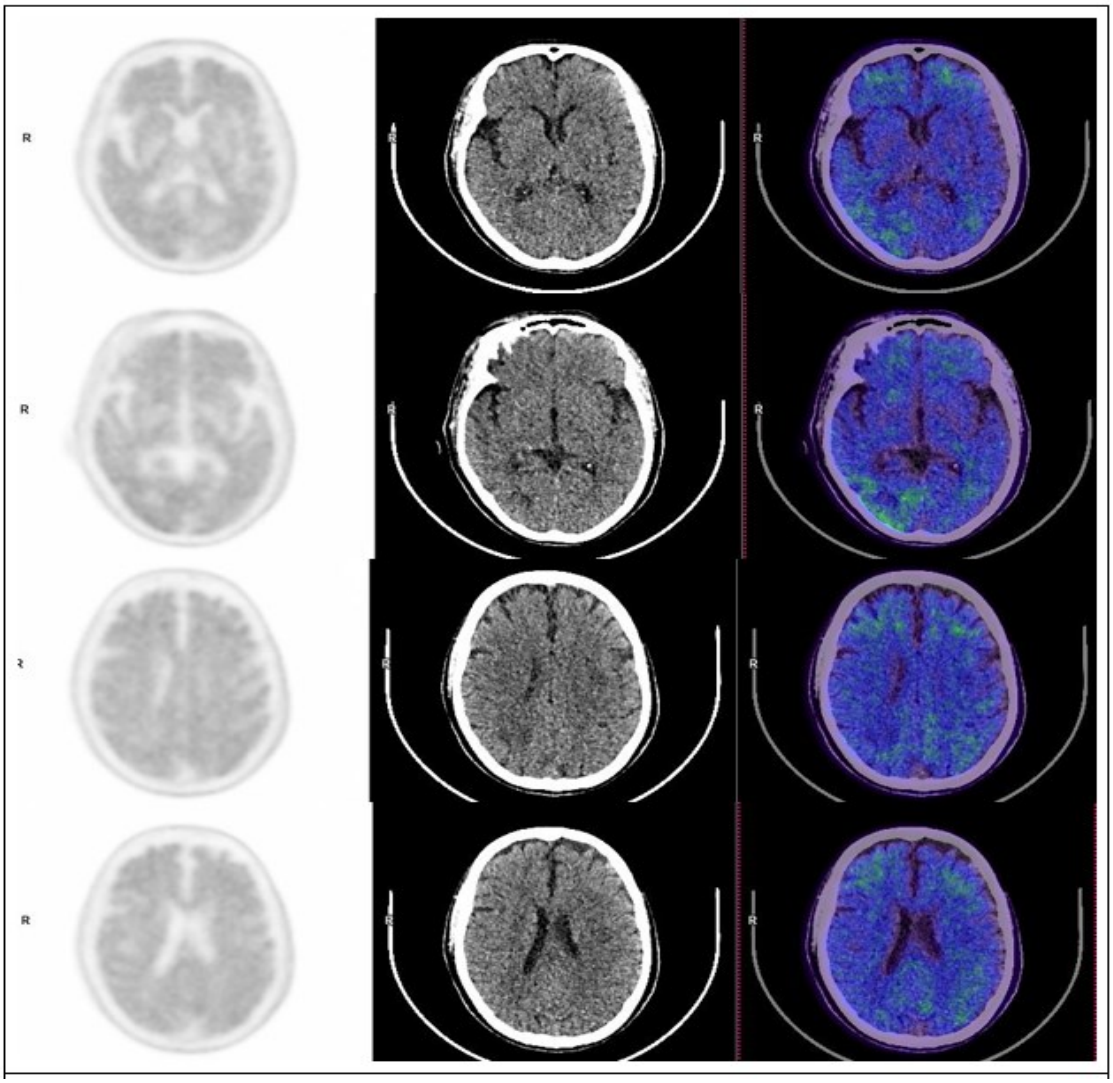

FIGURE 1. Case 1 - A Positive PET Amyloid scan

TABLE 2. Quantitative analysis using the standard uptake value ratios (SUVR) normalized to the cerebellar cortex

Regions of Interest (ROI)	Standard 90 minutes		Delayed scan	
	Mean SUV	SUVR normalized to the cerebellar cortex	Mean SUV	SUVR normalized to the cerebellar cortex
Anterior cingulate gyrus	1.54	1.64	1.39	1.65
Cerebellar cortex	0.94	-	0.84	-
Frontal lobe	1.77	1.88	1.61	1.92
Occipital lobe	2.05	2.18	1.89	2.25
Parietal lobe	1.97	2.1	1.78	2.12
Posterior cingulate gyrus	2.11	2.24	1.86	2.21
Temporal lobe	1.7	1.81	1.55	1.85

**An SUVR abnormality cut-off of 1.478 in a global cortical composite region relative to the cerebellar cortex was developed using histopathological confirmation as the standard of truth providing sensitivity (89.4%) and specificity (92.3%) to detect established Aß pathology [9].*

**Mean SUVs were acquired using auto-generated ROIs by molecular imaging neurology software provided by the PET manufacturer.*

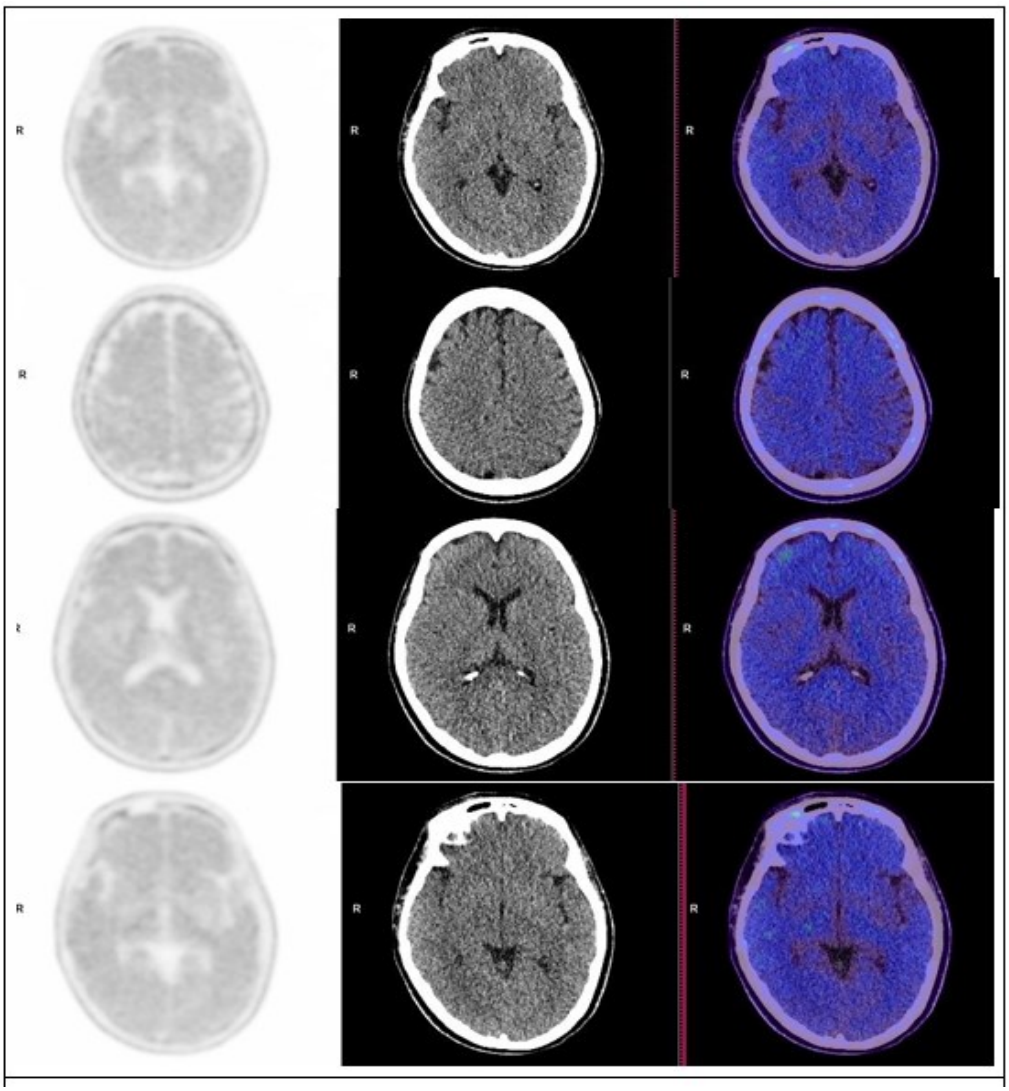

FIGURE 2. Case 2 - A Positive PET Amyloid scan

TABLE 3. Quantitative analysis using the standard uptake value ratios (SUVR) normalized to the cerebellar cortex

Regions of Interest (ROI)	Mean SUV	SUVR normalized to the cerebellar cortex**	SUVR normalized to the whole cerebellum***
Anterior cingulate gyrus	1.79	1.95	1.58
Frontal lobe	1.71	1.86	1.51
Occipital lobe	1.56	1.70	1.38
Parietal lobe	1.79	1.95	1.58
Posterior cingulate gyrus	1.86	2.02	1.65
Temporal lobe	1.72	1.87	1.52
Cerebellar cortex	0.92	-	-
Whole cerebellum	1.13	-	-

**Mean SUVs were acquired using auto-generated ROIs by molecular imaging neurology software provided by the PET manufacturer.*

***An SUVR abnormality cut-off of 1.478 in a global cortical composite region relative to the cerebellar cortex was developed using histopathological confirmation as the standard of truth providing sensitivity (89.4%) and specificity (92.3%) to detect established Aβ pathology [9].*

****Optimal SUVR cut-off for cerebellar gray matter is 1.43 and for whole cerebellum is 0.96 [10].*

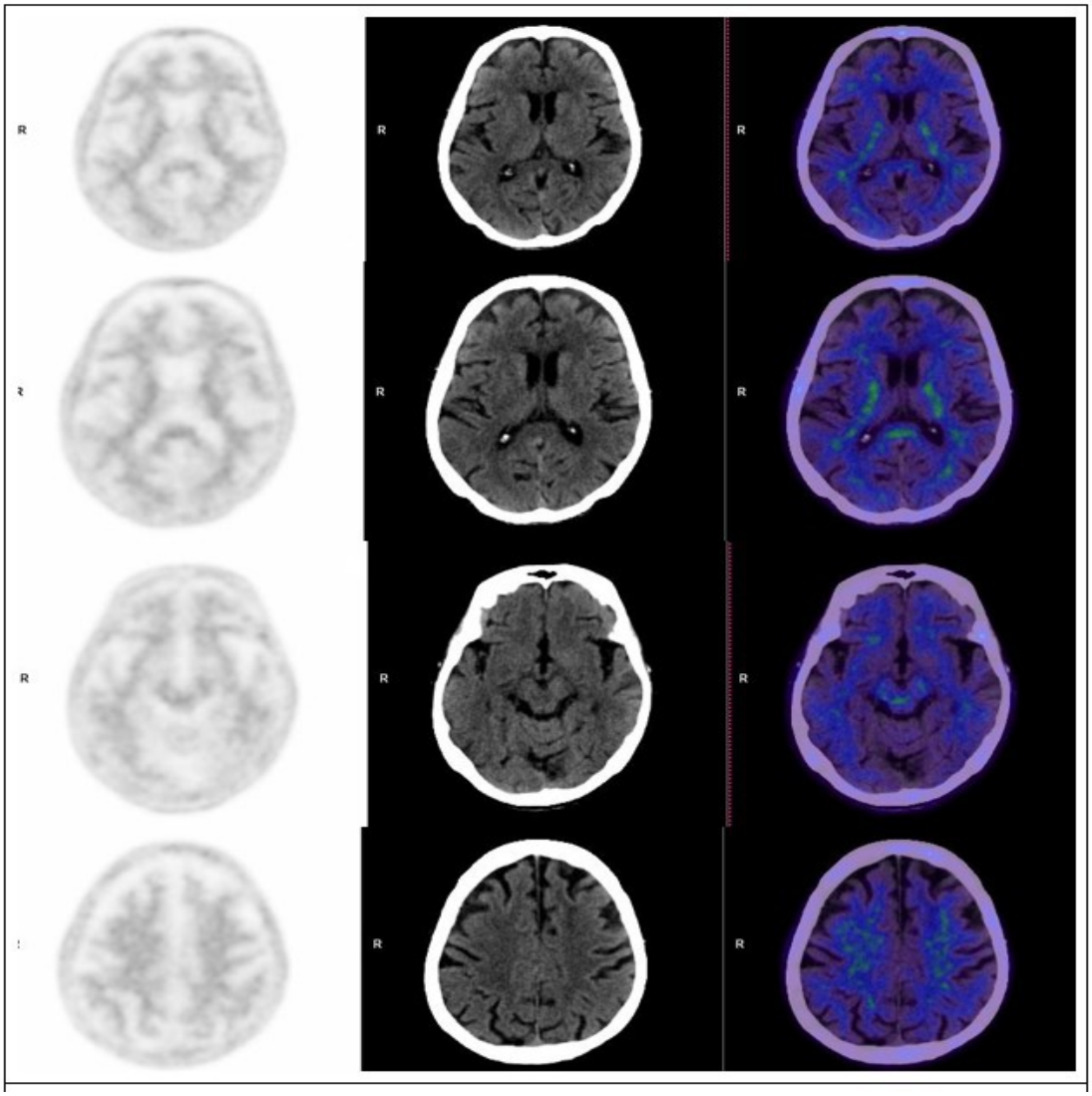

FIGURE 3. Case 3 - A Negative PET Amyloid scan showing non-specific Florbetaben uptake

TABLE 4. Quantitative analysis using the standard uptake value ratios (SUVR) normalized to the cerebellar cortex

Regions of Interest (ROI)	Mean SUV	SUVR normalized to the cerebellar cortex
Anterior cingulate gyrus	0.83	0.81
Cerebellar cortex	1.02	--
Frontal lobe	1.11	1.09
Occipital lobe	1.31	1.28
Parietal lobe	1.12	1.10
Posterior cingulate gyrus	1.30	1.27
Temporal lobe	1.20	1.18

**SUVR – standard uptake value ratio*

**An SUVR abnormality cut-off of 1.478 in a global cortical composite region relative to the cerebellar cortex was developed using histopathological confirmation as the standard of truth providing sensitivity (89.4%) and specificity (92.3%) to detect established Aβ pathology [9].*

**Mean SUVs were acquired using auto-generated ROIs by molecular imaging neurology software provided by the PET manufacturer.*

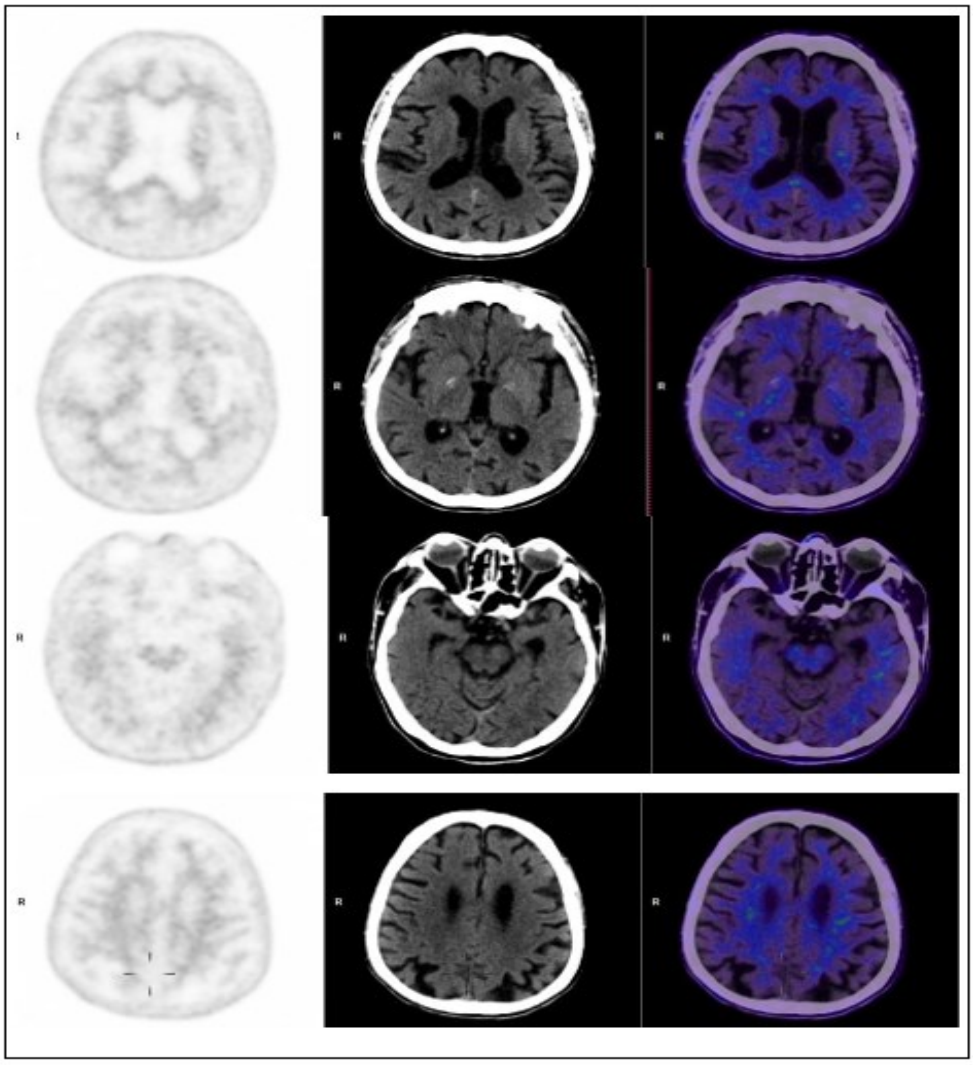

FIGURE 4. Case 4 - Negative for significant amyloid beta deposition

TABLE 5. Quantitative analysis using the standard uptake value ratios (SUVR) normalized to the cerebellar cortex

Regions of Interest (ROI)	Mean SUV	SUVR normalized to the cerebellar cortex	SUVR normalized to whole cerebellum
Anterior cingulate gyrus	0.73	1.04	0.73
Frontal lobe	0.87	1.24	0.87
Occipital lobe	0.98	1.4	0.98
Parietal lobe	0.88	1.26	0.88
Posterior cingulate gyrus	1.40	2.0	1.4
Temporal lobe	0.92	1.31	0.92
Cerebellar cortex	0.70	-	-
Whole cerebellum	1.00	-	-

**SUVR – standard uptake value ratio*

**An SUVR abnormality cut-off of 1.478 in a global cortical composite region relative to the cerebellar cortex was developed using histopathological confirmation as the standard of truth providing sensitivity (89.4%) and specificity (92.3%) to detect established Aß pathology [9].*

**Mean SUVs were acquired using auto-generated ROIs by molecular imaging neurology software provided by the PET manufacturer.*

the first amyloid PET scan in the country, the staff were given lectures to orient them with regards to the new tracer, its properties, and its indications.

The latest PET/CT scanner of both hospitals is the Siemens Biograph Vision 64 PET/CT scanner, already equipped with the necessary software application to process images acquired from the brain amyloid PET scan. The program is capable of processing the three F-18 amyloid tracers: F-18 florbetapir, florbetaben and flutemetamol despite having only F-18 florbetaben available for use in the country. The program itself is capable of generating automated regions of interest (ROIs) for the relevant regions in the brain where amyloid deposition is expected and provides standard uptake values (SUVs) and SUVRs.

Both institutions were able to administer uniform and correct radioactivity of the PET Amyloid tracer. Both were also able to image patients within the recommended 90 to 110 minute-uptake time and 20-minute acquisition time.

The AIT also recommends standardized interpretation protocols for interrater agreements. This must be set by the local professional certifying board. However, since these are the first four scans in the country, no preexisting data is available to set guidelines locally. Similar to other nuclear medicine procedures in the Philippines, protocols and references are derived from large, foreign organizations like the US FDA, SNMMI and EANM.

Diagnostic accuracy (clinical validity) of Florbetaben has been established by several studies [6, 10, 11, 12, 13]. The first amyloid tracer, C-11 Pittsburgh compound B has been the most extensively studied with proven good correlation with histopathological evidence of amyloid deposition. The F-18 based tracers flutemetamol and florbetapir have undergone tissue correlation and all three radiopharmaceuticals have been compared with C-11 PiB with good concordance [10, 11, 12,13]. F-18 Florbetaben is the first amyloid tracer studied in humans. Florbetaben's capability to increase probability of AD diagnosis has been supported by studies showing that it has high binding affinity to beta-amyloid plaques, concordant with thioflavin binding. It is not avid to α-synuclein in Lewy bodies or to tau lesions in postmortem cortices from dementia with Lewy bodies, Alzheimer's or FTLD patients. Several researches showed high Florbetaben uptake in the cortices of AD patients compared to patients with mild cognitive impairment and normal controls.

As with other elements of validation, each tracer and its associated interpretation protocol must be assessed separately. Since this is the first report of PET Amyloid Imaging in the Philippines, interpretation protocol has not yet been standardized. Clinical utility specific for Filipinos has also not been established locally.

Patients 1 and 2 had scans with visualized amyloid localization in the gray matter and with SUVRs higher than the 1.478 cut-off. Patient 1's amyloid PET scan reaffirmed the already known diagnosis of Alzheimer disease and objectively justified continuation of treatment. For Patient 2, the referring physician has started the patient on treatment for Alzheimer disease but wanted to increase the certainty of the clinical diagnosis. For the third and fourth patients, despite their advanced age, no significant amyloid deposition was noted. The negative brain amyloid PET scans discourage against dementia with amyloid deposition.patients who have histopathologically-proven amyloid

The 1.478 cut-off is derived from the study of Sabri et al. in 2015, a multicenter phase trial which used the similar PET scoring system recommended by the Neuraceq manufacturer [9]. It involved 218 patients (139 patients with AD, 5 with Dementia with Lewy bodies (DLB), 31 with other dementia disorders, 32 with non-dementia disorders and 11 who are cognitively normal). 74 of these patients had already died and whose brains became the autopsy — truth standard. Out of the 47 deposition, 44 of which had clinically-diagnosed AD. 46 out of 47 patients were read as PET amyloid positive scan. The three remaining positive scans were a case of DLB, one had another dementia disorder and one is not clinically diagnosed with dementia. This resulted in a sensitivity of 97.9% (95% CI 93.8-100%) and a specificity of 88.9% (95% CI 77.0–100%) for florbetaben PET imaging detection of amyloid plaques. Other studies have advocated an SUVR of 1.23 to 1.45.

Despite several studies suggesting using SUVRs, a study by Bullich et al. in 2016 involving 78 autopsied patients whose SUVRs were calculated from whole cerebellum and cerebellar cortical gray matter recommended that we prefer the use of visual assessment and limit the contribution of SUVRs in the interpretation of PET amyloid scans [13]. Subsequent research of two of the authors of this article stated that SUVRs were developed mainly to discriminate patients with amyloid-beta pathology from those who are cognitively normal hence they cannot be used to detect earliest amyloid deposition [10]. They however support SUVRs to increase the accuracy of non-expert readers who may

benefit from the additional contribution.

The procedure of PET Amyloid imaging is uniform for all of the four scans. One scan did not report SUVRs normalized to the whole cerebellum and one scan had delayed imaging due to patient motion. All four scans used visual assessment and SUVR quantification using the 1.478 cut-off.

RECOMMENDATIONS

For future PET Amyloid imaging as it is relatively new, the researchers would like to firstly highlight the importance of the appropriate use criteria set by AIT. The procedure is costly for the average Filipino, hence prudence should be exercised when requesting the test. Clinicians must weigh the pre-test and post-test probability and the expected benefit to their patient.

Second, institutions should always abide by the imaging guidelines to establish uniformity of the procedure. Interpretation confounders can arise starting from tracer administration up to interpretation.

We also recommend the reporting of SUVR cut-offs but primarily for future research purposes. To date, available studies regarding SUVR cut-offs employ them to support the findings of visual assessment which is the currently accepted method, and as a means of a semi-quantitative measurement. Calculating SUVRs based on both whole cerebellum and cerebellar cortex is also suggested until a local SUVR cut-off is established and validated.

REFERENCES

1. Alzheimer's Disease International, Wimo, A., Ali, G.-C., Guerchet, M., Prince, M., Prina, M., & Wu, Y.-T. (2015). World Alzheimer Report 2015: The global impact of dementia: An analysis of prevalence, incidence, cost and trends. https://www.alzint.org/resource/world-alzheimer-report-2015/.
2. Dominguez, J., Jiloca, L., Fowler, K. C., De Guzman, M. F., Dominguez-Awao, J. K., Natividad, B., Domingo, J., Dominguez, J. D., Reandelar, M., Jr, Ligsay, A., Yu, J. R., Aichele, S., & Phung, T. K. T. (2021). Dementia incidence, burden and cost of care: A Filipino community-based study. Frontiers in Public Health, 9, 628700. https://doi.org/10.3389/fpubh.2021.628700.
3. Suppiah, S., Didier, M.-A., & Vinjamuri, S. (2019). The who, when, why, and how of PET amyloid imaging in management of Alzheimer's disease-review of literature and interesting images. Diagnostics (Basel, Switzerland), 9 (2), 65. https://doi.org/10.3390/diagnostics9020065.
4. Park, M., & Moon, W.-J. (2016). Structural MR imaging in the diagnosis of Alzheimer's disease and other neurodegenerative dementia: Current imaging approach and future perspectives. Korean Journal of Radiology: Official Journal of the Korean Radiological Society, 17(6), 827. https://doi.org/10.3348/kjr.2016.17.6.827.
5. Ou, Y.-N., on behalf of Alzheimer's Disease Neuroimaging Initiative, Xu, W., Li, J.-Q., Guo, Y., Cui, M., Chen, K.-L., Huang, Y.-Y., Dong, Q., Tan, L., & Yu, J.-T. (2019). FDG-PET as an independent biomarker for Alzheimer's biological diagnosis: a longitudinal study. Alzheimer's Research & Therapy, 11(1). https://doi.org/10.1186/s13195-019-0512-1.
6. Johnson, K. A., Fox, N. C., Sperling, R. A., & Klunk, W. E. (2012). Brain imaging in Alzheimer disease. Cold Spring Harbor Perspectives in Medicine, 2(4), a006213. https://doi.org/10.1101/cshperspect.a006213.
7. Berti, V., Pupi, A., & Mosconi, L. (2011). PET/CT in diagnosis of dementia: PET/CT in diagnosis of dementia. Annals of the New York Academy of Sciences, 1228(1), 81–92. https://doi.org/10.1111/j.1749-6632.2011.06015.x
8. Johnson, K. A., Minoshima, S., Bohnen, N. I., Donohoe, K. J., Foster, N. L., Herscovitch, P., Karlawish, J. H., Rowe, C. C., Carrillo, M. C., Hartley, D. M., Hedrick, S., Pappas, V., & Thies, W. H. (2013). Appropriate use criteria for amyloid PET: a report of the Amyloid Imaging Task Force, the Society of Nuclear Medicine and Molecular Imaging, and the Alzheimer's Association. Journal of Nuclear Medicine: Official Publication, Society of Nuclear Medicine, 54(3), 476–490. https://doi.org/10.2967/jnumed.113.120618.
9. Sabri, O., Sabbagh, M. N., Seibyl, J., Barthel, H., Akatsu, H., Ouchi, Y., Senda, K., Murayama, S., Ishii, K., Takao, M., Beach, T. G., Rowe, C. C., Leverenz, J. B., Ghetti, B., Ironside, J. W., Catafau, A. M., Stephens, A. W., Mueller, A., Koglin, N., Hoffmann, A., … Florbetaben Phase 3 Study Group (2015). Florbetaben PET imaging to detect amyloid beta plaques in Alzheimer's disease: phase 3 study. Alzheimer's & dementia : the journal of the Alzheimer's Association, 11(8), 964–974. https://doi.org/10.1016/j.jalz.2015.02.004.
10. Bullich, S., Seibyl, J., Catafau, A. M., Jovalekic, A., Koglin, N., Barthel, H., Sabri, O., & De Santi, S. (2017). Optimized classification of 18F-Florbetaben PET scans as positive and negative using an SUVR quantitative approach and comparison to visual assessment. NeuroImage. Clinical, 15, 325–332. https://doi.org/10.1016/j.nicl.2017.04.025.
11. Johnson KA, Sperling RA, Gidicsin CM, et al. Florbetapir (F18-AV-45) PET to assess amyloid burden in Alzheimer's disease dementia, mild cognitive impairment, and normal aging. Alzheimers Dement. 2013;9:S72–83.
12. Richards, D., & Sabbagh, M. N. (2014). Florbetaben for PET imaging of beta-amyloid plaques in the brain. Neurology and Therapy, 3(2), 79–88.
13. Bullich, S., Catafau, A., Seibyl, J., & De Santi, S. (2016). Classification of positive and negative 18F-Florbetaben scans: Comparison of SUVR cutoff quantification and visual assessment performance. Journal of Nuclear Medicine, 57(supplement 2), 516.

Early versus Delayed Post-Therapy Whole Body Scintigraphy for Well-Differentiated Thyroid Carcinoma: a Meta-Analysis

Mary Amie Gelina E. Dumatol, MD, Jessica Elise A. Kuizon, MD, Michele D. Ogbac, MD

Nuclear Medicine Division, Philippine Heart Center
E-mail address: medumatol@alum.up.edu.ph

ABSTRACT

Introduction:

No clear consensus exists as to the optimal timing for conducting whole body scintigraphy (WBS) after radioactive iodine (RAI) therapy for differentiated thyroid carcinoma.

Objective:

This study aimed to compare the utility of early versus delayed post-therapy WBS in identifying residual lesions and metastases .

Methods:

A systematic review of existing literature was done, yielding 6 observational studies relevant to the subject. Meta-analyses were done comparing lesion detecting rates of early (3-4 days post-RAI) and delayed (7-11 days post-RAI) post-therapy WBS for thyroid remnants and metastases in the lymph nodes, lungs, and bone using a random-effects model with odds ratios (OR) and 95% confidence intervals (CIs). A subgroup analysis was also done relating to the type of collimator used in imaging.

Results:

There was no evidence to support that conducting WBS at either an early or delayed time after RAI therapy is superior to the other in detecting thyroid remnants (OR 1.11; 95% CI 0.86 – 1.42; p = 0.42), nodal (OR 1.01; 95% CI 0.74 – 1.38; p = 0.97), lung (OR 0.79; 95% CI 0.55 – 1.13; p = 0.20), and bone (OR 0.89; 95% CI 0.56 – 1.43; p = 0.64) metastases.

Conclusion:

There is no significant difference between early and delayed post-therapy whole body scintigraphy in terms of detecting thyroid remnants and nodal, lung, and bone metastases in patients with well-differentiated thyroid carcinoma.

Keywords*: post-therapy whole body scintigraphy (WBS), Iodine-131 (I-131), radioactive iodine (RAI) therapy, thyroid cancer*

INTRODUCTION

Thyroid cancer remains one of the most common malignancies worldwide, with a global incidence that is expected to continually rise throughout the coming years [1]. Differentiated thyroid carcinoma accounts for majority of thyroid malignancies [2], and among the mainstays of treatment for such cancers is total thyroidectomy with subsequent radioactive iodine (RAI) therapy. Therapy with iodine-131 (I-131) is given to achieve three main goals, namely 1) remnant ablation; 2) adjuvant treatment; and/or 3) treatment of known disease [3].

Whole body scintigraphy (WBS) after administration of therapeutic doses of I-131 for thyroid cancer is now often routinely performed as a means of demonstrating thyroid remnant uptake as well as presence and extent of metastatic disease. Indeed, compared to pre-therapy diagnostic scans that are commonly done after surgery, post-therapy WBS demonstrates increased sensitivity for for tumor localization and characterization, even showing improved detection of occult metastasis [4, 5].

However, debate remains as to the optimal time for conducting the post-therapy WBS. Though current clinical practice guidelines recommend doing WBS after RAI therapy and suggest conduction of such as early as 2 days to as late as 14 days after the date of therapy [6, 7, 8], a clear consensus has yet to be reached regarding the optimal timing of the scan. Previous observational studies aimed at determining when best to do the post-therapy WBS have had mixed conclusions, with some in favor of early imaging (i.e. 3-4 days after RAI) [9, 10] and others more for delayed imaging (i.e. 7-10 days after RAI) [11, 12], depending on which scanning time was able to reveal more detectable thyroid remnants and/or metastatic lesions.

Therefore, this meta-analysis aims to compare utility of the early and delayed post-therapy WBS in identifying residual lesion, locoregional, and distant metastases.

METHODS

This study was conducted in compliance with the guidelines set by the Meta-analyses of Observational Studies in Epidemiology (MOOSE) group (Appendix 1).

A. Search and selection process

Electronic databases (PubMed/MEDLINE, Google Scholar, and the Cochrane Library) were systematically searched for relevant articles from the date of publication up to December 2022.

A combination of the following terms was used in the search: “thyroid cancer” OR “thyroid carcinoma”, “post-therapy whole body scintigraphy” OR “post-therapy whole body scan” OR “WBS”, “iodine-131” OR “I-131”, AND “time” OR “early” AND “delayed”. Related articles were also manually searched, as were any gray literature and the reference lists of the preliminary yields.

Article titles and abstracts were then subjected to initial screening, and relevant articles subsequently underwent review of full texts. Any articles of which desired information was found to be ambiguous during the screening phase were automatically reviewed in full.

Inclusion criteria for studies were as follows: 1) study population of patients with well-differentiated thyroid cancer who underwent RAI therapy; 2) study population must have undergone both early and delayed post-therapy imaging; and 3) number of thyroid remnants and metastatic lesions reported and detected by experienced physician readers. Excluded from this analysis were case reports, reviews, editorials, and studies not written using the English language.

B. Data extraction and quality assessment

Data relevant to the study were extracted from the included articles by means of a thorough review. Information derived and thus reported include number of thyroid remnant lesions detected; number of metastatic lesions detected (nodal, lung, and/or bone, whichever were available); the study’s primary investigator; the year of publication; the country of origin; the total population of subjects; the mean age; the sex distribution; the diagnosis of the patients; the imaging hardware and type of collimator used for imaging; the mean administered dose for RAI; and the temporal definitions for early and delayed imaging.

The quality of the included studies was evaluated using the adapted Newcastle-Ottawa Quality Assessment Scale [13, 14]. Articles were evaluated based on selection, comparability of subjects, and outcome. The highest total score that could be achieved was 10. A score of at least 5 was considered satisfactory.

C. Data synthesis and statistical analysis

Statistical analyses were conducted using the Cochrane Review Manager program (Rev. Man. 5.4.1) [15]. Comparison of lesion detection rates for early and delayed imaging was done using odds ratios (OR) and 95% confidence intervals (CI). The Mantel-Haenzel method through a random-effects model was used in pooling the ORs across all the included studies for each outcome being measured. Two-tailed p values of < 0.05 were considered statistically significant for all analyses done. Heterogeneity among studies was evaluated using Cochran’s Q Chi-square test and I^2 statistics.

D. Sensitivity analysis and publication bias

Sensitivity analysis using the leave-one-out method was done to examine the effect of each included study on the overall results. Publication bias was assessed using the

Begg and Mazumdar rank correlation test and Egger's regression test via the jamovi software (version 1.6 MAJOR) [16].

RESULTS

A. Literature search

There were initially 55 studies identified from databases and manual searching. After duplication removal, 51 studies were kept for title and abstract screening as to the relevancy to the topic of interest. Subsequently, 38 studies were excluded, while 13 articles were sought for retrieval. Full text articles of 2 studies could not be found. The remaining 11 studies were assessed in full for eligibility. Of these, 2 studies were excluded because of different outcome measures presented; while 3 other studies were only available as conference abstracts that did not provide enough data for comprehensive analysis. Finally, a total of 6 studies were included in the meta-analysis. Figure 1 shows a schematic diagram of the study selection flow.

The included studies that encompassed post-therapy scans done from 2009 to 2022 report on a variety of detected lesions, namely number of thyroid remnants and metastatic lesions in the lymph nodes, lungs, and bones, with individual studies accounting for all or a select combination of the aforementioned. The 6 studies, a majority of which were conducted in Asian countries, involved a total of 691 patients with well-differentiated thyroid cancer who underwent RAI therapy with administered doses ranging from 1110 – 9250 megabecquerels (MBq). For these studies, early imaging was done 3-4 days after RAI, while delayed imaging was done 7-11 days after RAI. Five studies made use of dual-head gamma cameras. A summary of the characteristics of the included studies is shown in Table 1.

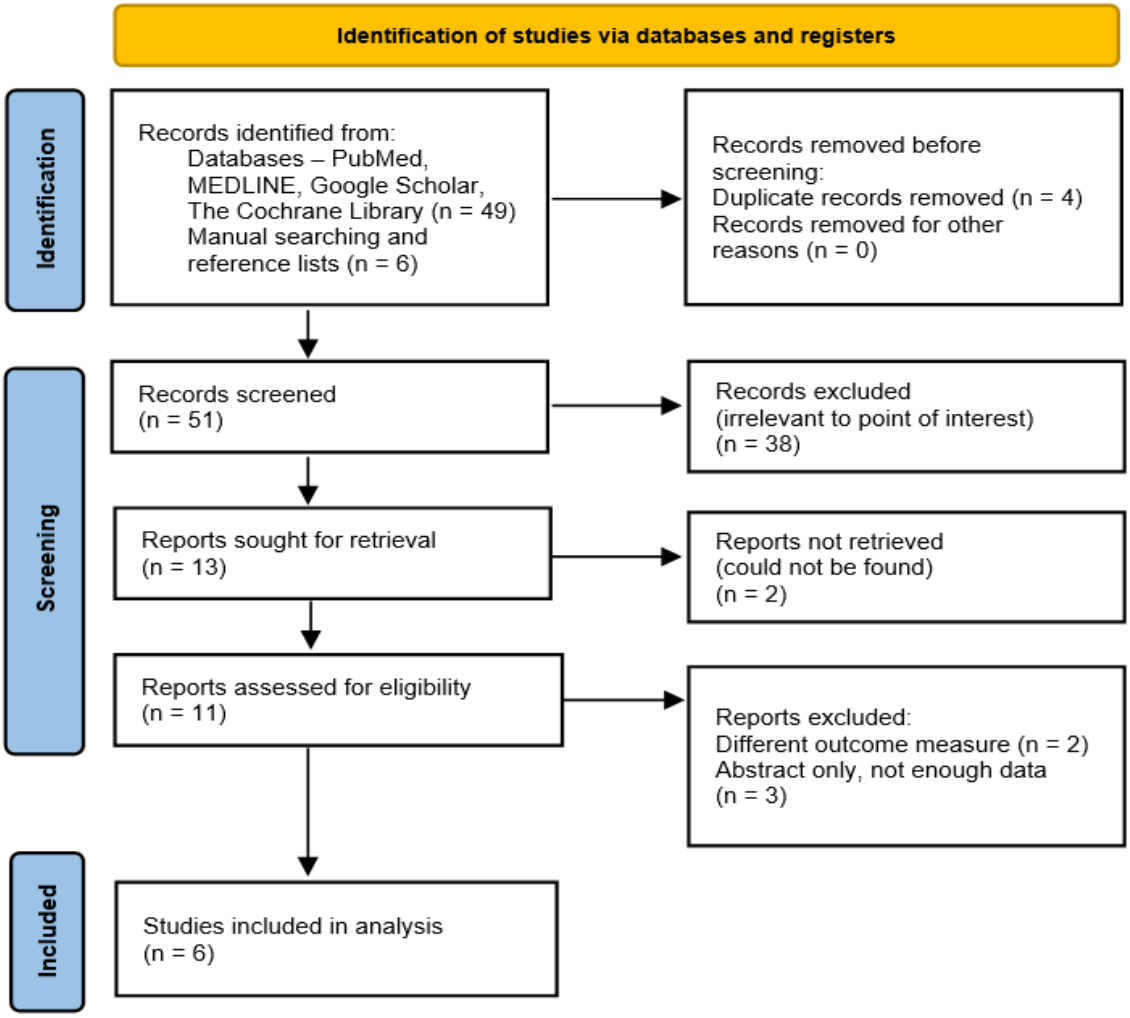

FIGURE 1. Schematic diagram of the study selection process

TABLE 1. Study characteristics of the included studies

Author (Year)	Country	Design	N (M/F)	Thyroid CA PTC/FTC	Mean RAI Activity	Mean Age	Early Imaging	Delayed Imaging	Hardware (Collimator)	Lesions Reported
Liu et al. (2022) [17]	China	Retrospective	161 (68/93)	152/9	3700 – 7400 MBq (100 – 200 mCi)	44.75 ± 14.43	3 days	7 days 10 days	SPECT/CT – Siemens Symbia T2 (HEPH)	Remnants, Nodal, Lung
Salvatori et al. (2013) [18]	Italy	Retrospective	134 (31/103)	123/11	3700 – 7400 MBq (100 – 200 mCi)	51 ± 16	3 days	7 days	Dual head – [unspecified] (HEPH)	Remnants, Nodal, Lung, Bone
Kodani et al. (2012) [19]	Japan	Retrospective	24 (10/14)	21/3	1850 – 3700 MBq (50 – 100 mCi)	61	3 days	7-9 days	Dual head – Philips PRISM 2000XP (HEPH)	Remnant, Lung, Bone
Lee et al. (2011) [10]	South Korea	Retrospective	81 (14/67)	79/2	3700 – 7400 MBq (100 – 200 mCi)	52 ±13	3 days	10 days	Dual head – ADAC Vertex V60 (MEPH)	Remnants *Unspecified Metastases
Chong et al. (2010) [11]	South Korea	Retrospective	52 (16/36)	45/7	5550 – 9250 MBq (150 – 250 mCi)	54 ±16	3 days	7 days	Dual head - GE Millennium VG (MEPH)	Lung, Bone
Hung et al. (2009) [9]	Taiwan	Retrospective	239 (67/172)	205/34	1110 – 7400 MBq (30 – 200 mCi)	45.8 ± 15	3-4 days	10-11 days	Dual head - GE VariCAM (MEPH)	Remnants, Nodal, Lung, Bone

Legend: *PTC - papillary thyroid carcinoma; FTC - follicular thyroid carcinoma; HEPH – high-energy parallel hole collimator; MEPH – medium-energy parallel hole collimator*

TABLE 2. Study quality assessment of the included studies based on the Newcastle-Ottawa criteria

	SELECTION				COMPARABILITY of subjects in different groups on basis of design or analysis with confounding factors	OUTCOME		Total Scores
	Representativeness of cases	Sample size	Non-respondents	Exposure ascertainment / Risk factor		Ascertainment of outcome	Statistical Test	
Liu et al. (2022) [17]	*		*	*	**	**	*	8
Salvatori et al. (2013) [18]	*		*	*	**	**	*	8
Kodani et al. (2012) [19]	*		*	*	**	**	*	8
Lee et al. (2011) [10]	*		*	*	**	**	*	8
Chong et al. (2010) [11]	*		*	**	**	**	*	9
Hung et al. (2009) [9]	*		*	*	**	**	*	8

B. Quality assessment

Quality assessment of the studies using the Newcastle-Ottawa scale resulted in scores ranging from 8-9, indicating adequate and overall good quality of study methodology. (Table 2)

C. Meta-analysis of included studies

Thyroid Remnants

Five of the 6 included studies reported detected thyroid remnant lesions using post-therapy WBS at both early and delayed imaging times for a total of 639 patients with well-differentiated thyroid cancer. Among the 639 patients, early imaging detected 465 thyroid remnant lesions (73%) while 452 lesions (71%) were detected using delayed imaging. Figure 2 demonstrates that there is no evidence to support that conducting post-therapy WBS at either an early or delayed time is superior to the other in detecting thyroid remnant lesions (OR 1.11; 95% CI 0.86 – 1.42; p = 0.42). Low heterogeneity was noted in the analysis of thyroid remnant detection (I^2= 0%; Tau^2 = 0.00; p = 0.83).

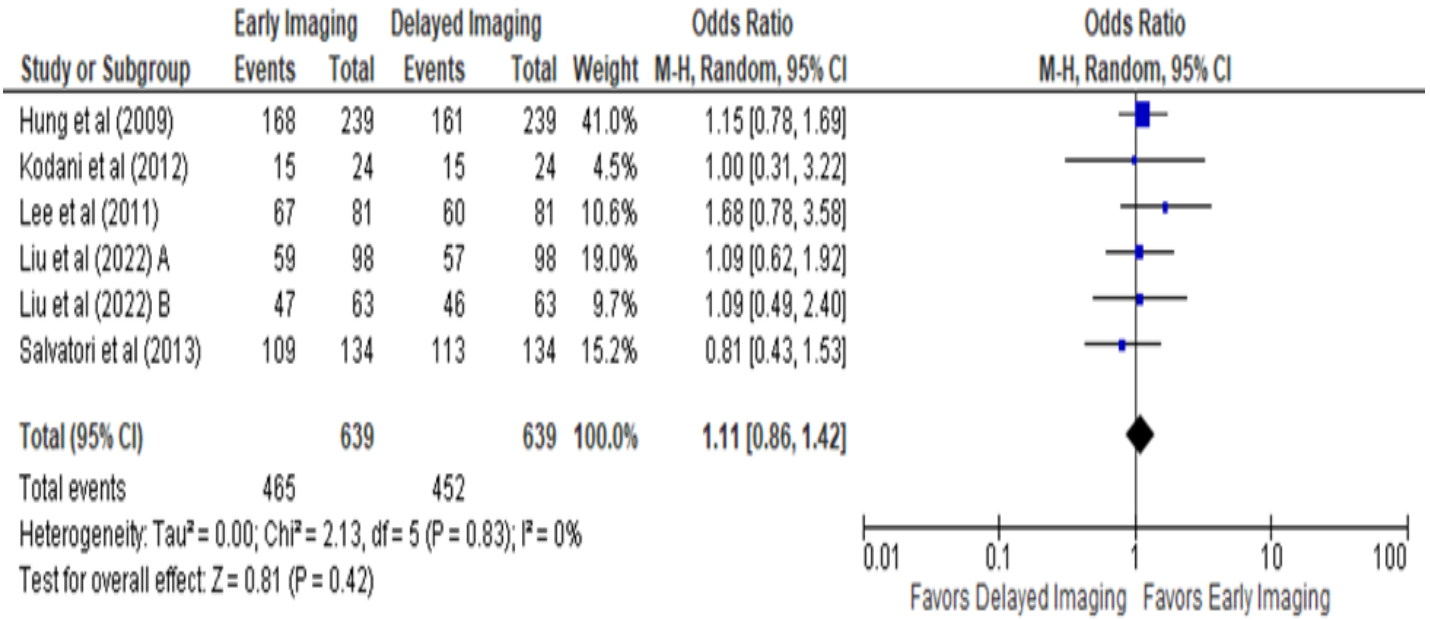

FIGURE 2. Thyroid remnants meta-analysis of early and delayed post-therapy WBS

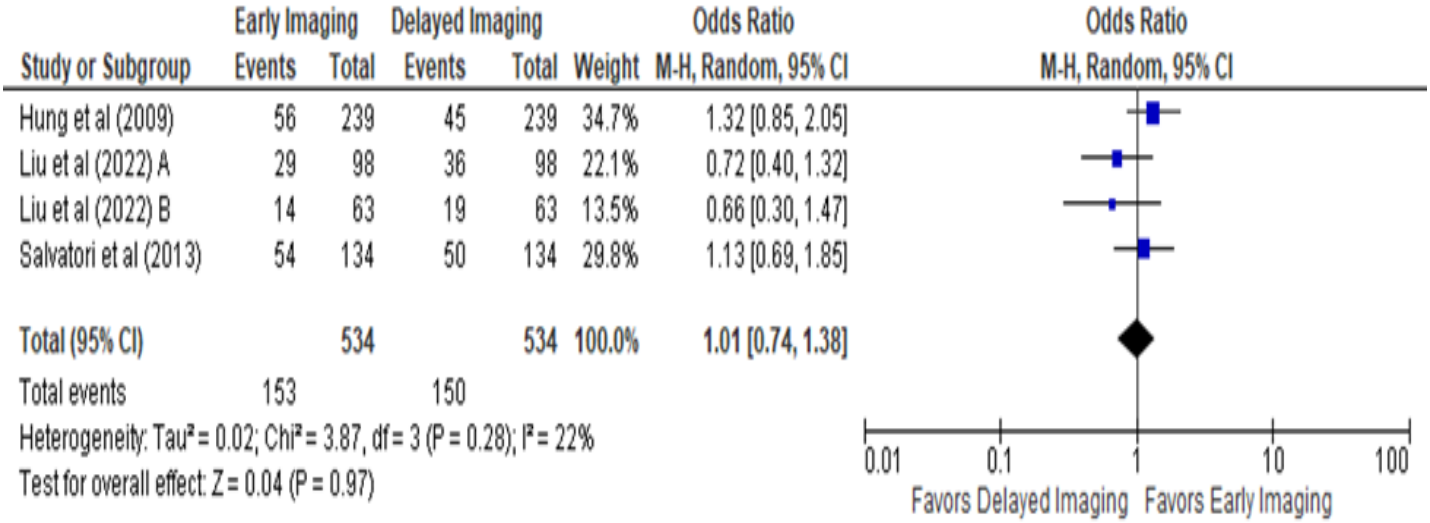

FIGURE 3. Nodal metastases meta-analysis of early and delayed post-therapy WBS

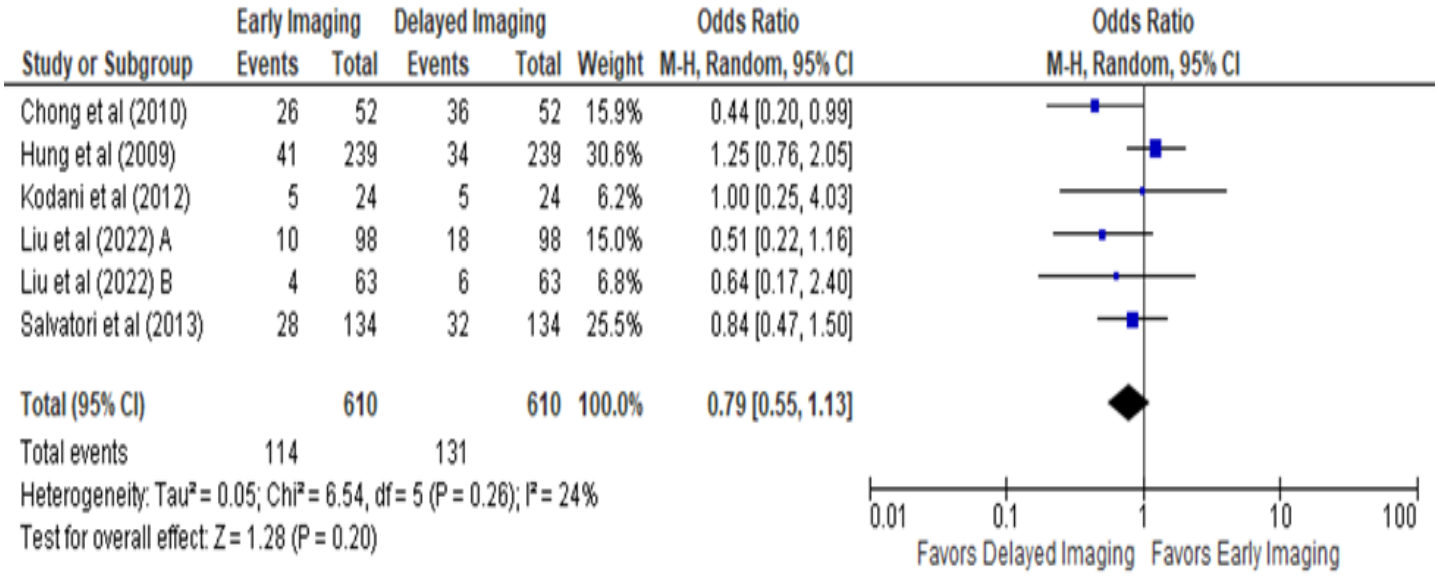

FIGURE 4. Lung metastases meta-analysis of early and delayed post-therapy WBS

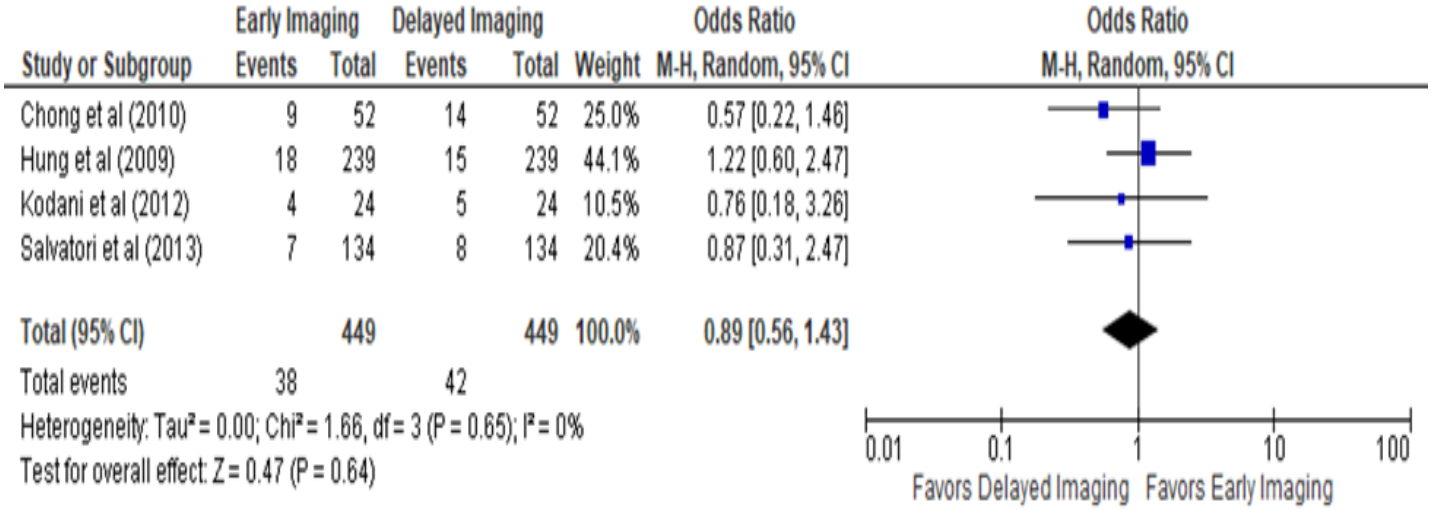

FIGURE 5. Bone metastases meta-analysis of early and delayed post-therapy WBS

Nodal Metastases

Among the six included studies, there were 3 studies that reported detected nodal metastatic lesions, particularly cervical and mediastinal lymph nodes, using post-therapy WBS at both early and delayed imaging times. Of the 534 patients with well-differentiated thyroid cancer involved in this analysis, early imaging detected 153 nodal metastases (29%) while 150 lesions (28%) were detected using delayed imaging. Figure 3 shows that there is no evidence to support that conducting WBS at either an early or delayed time after RAI therapy is superior to the other in detecting nodal metastatic lesions (OR 1.01; 95% CI 0.74–1.38; p = 0.97). Low heterogeneity was noted in the analysis of nodal metastasis detection (I^2= 22%; Tau^2 = 0.02; p = 0.28).

Lung Metastases

Lung metastatic lesions detected using post-therapy WBS at both early and delayed imaging times were reported in 5 of 6 included studies, involving a total of 610 thyroid carcinoma patients who underwent RAI therapy. Early imaging was able to detect 114 lung metastases (19%), while delayed imaging detected 131 lesions (21%). Figure 4 shows that there is no evidence to support that conducting WBS at either an early or delayed time after RAI therapy is superior to the other in detecting lung metastases (OR 0.79; 95% CI 0.55 – 1.13; p = 0.20). Low heterogeneity was noted in the analysis of lung metastasis detection (I^2= 24%; Tau^2 = 0.05; p = 0.26).

TABLE 3. Subgroup analysis of detected thyroid remnant and metastatic lesions based on collimator

	Thyroid Remnant		Nodal Metastases		Lung Metastases		Bone Metastases	
	OR (95% CI)	***p***	**OR (95% CI)**	***p***	**OR (95% CI)**	***p***	**OR (95% CI)**	***p***
HEPH	0.98 (0.69, 1.41)	0.93	0.89 (0.63, 1.25)	0.49	0.73 (0.48, 1.11)	0.14	0.83 (0.36, 1.94)	0.67
MEPH	1.24 (0.88, 1.75)	0.22	-	-	0.78 (0.29, 2.14)	0.63	0.89 (0.43, 1.85)	0.75

Bone Metastases

There were 4 out of the 6 included studies that reported on detected bone metastatic lesions using post-RAI therapy scans at both early and delayed imaging times. This analysis involved 449 patients with well—differentiated thyroid cancer, and among them, early imaging detected 38 bone metastatic lesions (8%) while 42 lesions (9%) were detected using delayed imaging. Figure 5 demonstrates that there is no evidence to support that conducting WBS at either an early or delayed time is superior to the other in detecting bone metastases (OR 0.89; 95% CI 0.56 – 1.43; p = 0.64). Low heterogeneity was noted in the analysis of bone metastasis detection (I^2= 0%; Tau^2 = 0.00; p = 0.65).

D. Subgroup analysis

Subgroup analysis was done based on the type of collimator used in performing the post-therapy WBS. There were 3 studies that used high-energy parallel hole (HEPH) collimators, while the other 3 studies made use of medium-energy parallel hole (MEPH) collimators. There is no evidence to support that conducting WBS at either an early or delayed time is superior to the other in detecting thyroid remnants as well as nodal, lung, and bone metastatic lesions (all p values >0.05) for both the HEPH and the MEPH groups. The results of the subgroup analysis according to collimator used are summarized in Table 3.

E. Sensitivity analysis and publication bias

None of the studies were determined to be overly influential on the results of the analyses conducted. Neither the rank correlation nor the regression tests suggested strong evidence for publication bias for all the meta-analyses done (all p values > 0.05).

DISCUSSION

The utility of post-therapy whole body scintigraphy (WBS) has been attested to by several studies with its superior sensitivity that allows the detection of more tumors and metastases than would pre-therapy diagnostic scans [20, 21]. Such information would contribute to prognostication and management of patients with thyroid carcinoma, guiding clinicians as to which patients would need further diagnostic imaging, closer monitoring, repeat radioactive iodine (RAI) therapy, and even other forms of treatment outside RAI [20, 22].

The question remains, however, whether there exists an ideal time for conducting the post-therapy WBS. As in any scintigraphic study, proper timing is crucial in obtaining quality images. Imaging early may avoid missing lesions due to washout [9], but a longer delay helps in achieving optimal target-to-background ratios, which may also improve lesion detection [21]. Because the presence of a single metastatic lesion is enough to change the staging and prognosis of a patient, as well as influence monitoring and management, the ability of I-131 whole body scintigraphy in detection of such lesions must be optimized. Therefore, this meta-analysis aims to compare early versus delayed imaging in well-differentiated thyroid carcinoma patients who received RAI therapy in terms of lesion detection rate. To the best knowledge of the researchers, this is the first attempt made in this matter.

Based on the results of the conducted analyses, there is currently no evidence to support that early or delayed post-therapy WBS was superior to the other in identifying thyroid remnants as well as metastatic lesions in the lymph nodes, lungs, and bones. Subgroup analysis according to the type of collimator used, whether

high-energy parallel hole (HEPH) or medium-energy parallel hole (MEPH), likewise revealed no statistically significant difference between lesion detection rates of early and delayed scanning across all 4 sites analyzed.

Although no evident overall difference was demonstrated in thyroid remnant and metastatic lesion detection rates of early and delayed post-therapy WBS, these results should be interpreted while factoring in certain conditions. Firstly, the influence of using single photon emission computed tomography (SPECT) was not assessed, given that it was utilized in only one of the included studies [17]. The addition of SPECT, particularly when combined with computed tomography (CT), has been shown to be beneficial in the post-RAI setting by improving lesion detection and increasing confidence in diagnostic interpretation [23, 24], compared to planar scintigraphy alone. Additionally, the effect of previous RAI therapy was likewise not explored. In a study by Oh et al. [25], there were considerable differences in the diagnostic performances of the post-therapy WBS in patients who have undergone multiple RAI therapies compared to those on their first treatment session, with the latter showing greater sensitivity and specificity than the former.

Proper patient preparation is vital to the satisfactory conduction of any diagnostic test as well as the success of any treatment procedure. For instance, following a low iodine diet prior to RAI administration has been shown to be associated with an increase in remnant uptake [26]. Not all studies included in this analysis had mention of the kind of patient preparation done as well as the uniformity of preparation across patients (i.e. whether all patients were compliant, and for how long); and this may influence whether certain lesions may be more visible on scanning or remain undetected.

In relation to other pretreatment processes that may affect tracer uptake, most of the included studies in this analysis did not mention whether patients underwent diagnostic WBS prior to RAI therapy or not. Pre-therapy WBS has been postulated to cause thyroid stunning and though much controversy still exists regarding this phenomenon, it has been associated with variable degrees of reduced iodine-131 (I-131) uptake on the post -therapy scan [27]. It is uncertain whether this may have affected detection rates on the scans involved in this analysis.

Furthermore, it should be noted that the visual interpretation of a diagnostic scan such as the post-therapy WBS may be influenced by several factors including but not limited to individual reader experience and fatigue, individual patient characteristics such as co-morbidities, technical aspects affecting image quality,

and availability of other diagnostic test results for correlation. Several non-thyroid conditions may also manifest with I-131 tracer uptake and thus, potentially cause false positive scan interpretation [28].

This study possesses several limitations. There were only a limited number of studies derived, of which a number had small sample sizes. Included only were studies written in the English language. This study also focused primarily on lesion detection rate involving thyroid remnants and nodal, lung, and bone metastases, and did not account for the intensity of uptake of such lesions. Lesion detection was based mostly on the ability of expert physician readers in interpreting the scans. Not all the studies did confirmatory work-up via pathologic biopsy or correlation with anatomic imaging, such as computed tomography (CT) and magnetic resonance imaging (MRI). Finally, the imaging hardware and protocols used were varied across the studies included, depending on specific country guidelines, respective institutional preferences, and equipment availability.

CONCLUSION

This meta-analysis did not show a significant difference between early and delayed post-therapy whole body scintigraphy in terms of detecting thyroid remnants and nodal, lung, and bone metastases in patients with well-differentiated thyroid carcinoma. This finding supports the recommended timing range provided by current practice guidelines.

Acknowledgment

The researchers would like to thank Dr. Irene Bandong for her valuable feedback in shaping this manuscript to its final form.

REFERENCES

1. Shank JB, Are C, Wenos CD. Thyroid cancer: Global burden and trends. Indian Journal of Surgical Oncology. 2021;13 (1):40–5.
2. Jukkola A, Bloigu R, Ebeling T, Salmela P, Blanco G. Prognostic factors in differentiated thyroid carcinomas and their implications for current staging classifications. Endocrine-Related Cancer. 2004Sep;11(3):571–9.
3. Van Nostrand D. Selected controversies of Radioiodine Imaging and therapy in differentiated thyroid cancer. Endocrinology and Metabolism Clinics of North America. 2017Jun29;46(3):783–93.
4. Bartel (Chair) TB, Magerefteh S, Avram AM, Balon HR, De Blanche LE, Dadparvar S, et al. SNMMI procedure standard for scintigraphy for differentiated thyroid cancer. Journal of Nuclear Medicine Technology. 2020Sep;48 (3):202–9.
5. Luster M, Clarke SE, Dietlein M, Lassmann M, Lind P, Oyen WJ, et al. Guidelines for radioiodine therapy of differentiated thyroid cancer. European Journal of Nuclear Medicine and Molecular Imaging. 2008;35(10):1941–59.
6. Haugen BR, Alexander EK, Bible KC, Doherty GM, Mandel SJ, Nikiforov YE, et al. 2015 American Thyroid Association Management Guidelines for adult patients with thyroid nodules and differentiated thyroid cancer: The American Thyroid Association Guidelines Task Force on thyroid nodules and differentiated thyroid cancer. Thyroid. 2016Jan12;26(1):1–133.
7. Pacini F, Fuhrer D, Elisei R, Handkiewicz-Junak D, Leboulleux S, Luster M, et al. 2022 ETA consensus statement: What are the indications for post-surgical radioiodine therapy in differentiated thyroid cancer? European Thyroid Journal. 2022;11(1).
8. Department of Health, Republic of the Philippines. The Philippine Interim Clinical Practice Guidelines for the Diagnosis and Management of Well-Differentiated Thyroid Cancer 2021. [Internet, last updated April 2022, accessed December 2022]. Available from https://doh.gov.ph/dpcb/doh-approved-cpg.
9. Hung B-T, Huang S-H, Huang Y-E, Wang P-W. Appropriate time for post-therapeutic I-131 whole body scan. Clinical Nuclear Medicine. 2009Jun;34(6):339–42.
10. Lee JW, Lee SM, Koh GP, Lee DH. The comparison of 131-I whole-body scans on the third and tenth day after 131I therapy in patients with well-differentiated thyroid cancer: Preliminary report. Annals of Nuclear Medicine. 2011;25(6):439–46.
11. Chong A, Song H-C, Min J-J, Jeong SY, Ha J-M, Kim J, et al. Improved detection of lung or bone metastases with an I-131 whole body scan on the 7th day after high-dose I-131 therapy in patients with thyroid cancer. Nuclear Medicine and Molecular Imaging. 2010;44(4):273–81.
12. Agrawal K, Bhattacharya A, Raja S, Sood A, Mittal B. Utility of delayed post-therapy whole body I-131 scan over early scan in patients with differentiated thyroid cancer: A prospective study. Journal of Nuclear Medicine. 2013May;54(S2).
13. Wells G, Shea B, O'Connell D, Peterson J, Welch V, Losos M, Tugwell P: The Newcastle-Ottawa Scale (NOS) for assessing the quality of nonrandomised studies in meta-analyses [Internet]. Ottawa Hospital Research Institute; 2013 [accessed 2022 December]. Available from http://www.ohri.ca/programs/clinical_epidemiology/oxford.asp.
14. Herzog R, Álvarez-Pasquin MJ, Díaz C, Del Barrio JL, Estrada JM, Gil Á. Are Healthcare Workers' intentions to vaccinate related to their knowledge, beliefs and attitudes? A systematic review. BMC Public Health. 2013;13(1).
15. The Cochrane Collaboration. Review Manager (RevMan) [Computer program]. Version 5.4. 2020.
16. The jamovi project. jamovi. [Computer program]. Version 5.4. 2021 .
17. Liu S, Zuo R, Yang T, Pang H, Wang Z. A semiquantitative study of the optimal whole-body imaging time after 131I therapy for differentiated thyroid cancer. Frontiers in Endocrinology. 2022;13.
18. Salvatori M, Perotti G, Villani MF, Mazza R, Maussier ML, Indovina L, et al. Determining the appropriate time of execution of an I-131 post-therapy whole-body scan. Nuclear Medicine Communications. 2013Sep;34(9):900–8.
19. Kodani N, Okuyama C, Aibe N, Matsushima S, Yamazaki H. Utility of additional delayed post-therapeutic 131I whole-body scanning in patients with thyroid cancer. Clinical Nuclear Medicine. 2012Mar;37(3):264–7.
20. Amdur RJ, Mazzaferri EL. The value of a post-treatment whole body scan. Essentials of Thyroid Cancer Management. 2005;:65–8.
21. Bravo PE, Goudarzi B, Rana U, Filho PT, Castillo R, Rababy C, et al. Clinical significance of discordant findings between pre-therapy 123 I and post-therapy 131 I whole body scan in patients with thyroid cancer. International Journal of Clinical and Experimental Medicine. 2013;6:320 –333.
22. Obaldo JM, Ogbac RV. Value of post-therapy whole body scintigraphy in predicting the need for subsequent radioactive iodine therapy in patients with well-differentiated thyroid carcinoma. Acta Medica Philippina. 2009;43(4):69–75.
23. Hassan FU, Mohan HK. Clinical utility of SPECT/CT Imaging Post-Radioiodine therapy: Does it enhance patient management in thyroid cancer? European Thyroid Journal. 2015Jul31;4(4):239–45.

24. Maruoka Y, Abe K, Baba S, Isoda T, Sawamoto H, Tanabe Y, et al. Incremental diagnostic value of SPECT/CT with131I scintigraphy after radioiodine therapy in patients with well-differentiated thyroid carcinoma. Radiology. 2012 Dec 1;265(3):902–9.
25. Oh J-R, Byun B-H, Hong S-P, Chong A, Kim J, Yoo S-W, et al. Comparison of 131i whole-body imaging, 131I SPECT/CT, and 18F-FDG PET/CT in the detection of metastatic thyroid cancer. European Journal of Nuclear Medicine and Molecular Imaging. 2011Apr20;38(8):1459–68.
26. Dobrenic M, Huic D, Zuvic M, Grosev D, Petrovic R, Samardzic T. Usefulness of low iodine diet in managing patients with differentiated thyroid cancer - initial results. Radiology and Oncology. 2011;45(3).
27. Kalinyak JE, McDougall IR. Whole-body scanning with radionuclides of iodine, and the controversy of “thyroid stunning.” Nuclear Medicine Communications. 2004;25 (9):883–9.
28. Oral A, Yazıcı B, Eraslan C, Burak Z. Unexpected false-positive I-131 uptake in patients with differentiated thyroid carcinoma. Molecular Imaging and Radionuclide Therapy. 2018;27(3):99–106.

Appendix 1: MOOSE Checklist for Meta-analyses of Observational Studies

Item No	Recommendation	Reported on Page No
Reporting of background should include		
1	Problem definition	3
2	Hypothesis statement	-
3	Description of study outcome(s)	3
4	Type of exposure or intervention used	3
5	Type of study designs used	3-4
6	Study population	3-4
Reporting of search strategy should include		
7	Qualifications of searchers (eg, librarians and investigators)	Title, 4
8	Search strategy, including time period included in the synthesis and key words	4
9	Effort to include all available studies, including contact with authors	4
10	Databases and registries searched	4
11	Search software used, name and version, including special features used (eg, explosion)	4
12	Use of hand searching (eg, reference lists of obtained articles)	4
13	List of citations located and those excluded, including justification	4
14	Method of addressing articles published in languages other than English	-
15	Method of handling abstracts and unpublished studies	4
16	Description of any contact with authors	-
Reporting of methods should include		
17	Description of relevance or appropriateness of studies assembled for assessing the hypothesis to be tested	3-4
18	Rationale for the selection and coding of data (eg, sound clinical principles or convenience)	3-4
19	Documentation of how data were classified and coded (eg, multiple raters, blinding and interrater relia-	3-4
20	Assessment of confounding (eg, comparability of cases and controls in studies where appropriate)	-
21	Assessment of study quality, including blinding of quality assessors, stratification or regression on possible predictors of study results	4-5
22	Assessment of heterogeneity	5
23	Description of statistical methods (eg, complete description of fixed or random effects models, justification of whether the chosen models account for predictors of study results, dose-response models, or cumulative meta-analysis) in sufficient detail to be replicated	5
24	Provision of appropriate tables and graphics	6-7;
Reporting of results should include		
25	Graphic summarizing individual study estimates and overall estimate	6-7;
26	Table giving descriptive information for each study included	7,
27	Results of sensitivity testing (eg, subgroup analysis)	10-11
28	Indication of statistical uncertainty of findings	8-11

Item No	Recommendation	Reported on Page
Reporting of discussion should include		
29	Quantitative assessment of bias (eg, publication bias)	11
30	Justification for exclusion (eg, exclusion of non-English language citations)	13
31	Assessment of quality of included studies	7
Reporting of conclusions should include		
32	Consideration of alternative explanations for observed results	11-12
33	Generalization of the conclusions (ie, appropriate for the data presented and within the domain of the	11-12
34	Guidelines for future research	-
35	Disclosure of funding source	-

From: Stroup DF, Berlin JA, Morton SC, et al, for the Meta-analysis Of Observational Studies in Epidemiology (MOOSE) Group. Meta-analysis of Observational Studies in Epidemiology. A Proposal for Reporting. *JAMA*. 2000;283(15):2008-2012. doi: 10.1001/jama.283.15.2008.

ARAMAX SOLUTIONS INC.

PET/CT . CYCLOTRON . LINAC . X-RAY. PACS SYSTEM

CYCLOTRON

PET/CT

PRODUCTS

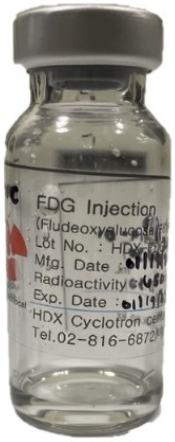

FDG

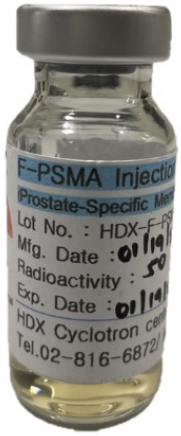

F-PSMA

OUR OWN CENTER

PERPETUAL HELP
MEDICAL CENTER - LAS PIÑAS

Chinese General Hospital
and Medical Center

Cebu Doctors'
University Hospital

DAVAO ONE WORLD
DIAGNOSTIC CENTER, INC.

Prime Health
IMAGING P.E.T./C.T.SCAN CENTER
In Shaw Boulevard

Prime Health
IMAGING P.E.T./C.T.SCAN CENTER
In Franca Arcade

ADDRESS

1702 ANNAPOLIS WILSHIRE PLAZA, #11 ANNPOLIS ST.,GREENHILLS, SAN JUAN 1502

CONTACT INFORMATION

Tel.: (02) 8526-8347
Email: aramaxsolutions@gmail.com

KHealth
Bring good things to life

CAREVIEW

Taking the Lead in PET/CT Imaging and Innovative Radiopharmaceuticals

OUR MANAGED PET/CT CENTERS

[18F]-FDG

A sugar analog used to **detect metabolically active malignant lesions.** A non-invasive approach to accurate diagnosis and staging for the optimal management of cancer patients

[18F]-FBB

Developed for routine clinical application to visualize beta amyloid neuritic plaque density. An effective tool to **differentiate Alzheimer's Disease** from other forms of Dementia

Khealth: The only licensed manufacturer of

[18F]-FPSMA

Named as a top medical innovation by Cleveland Clinic in 2022. PSMA PET scan has greater sensitivity and can **detect prostate cancer metastases** sooner, allowing clinicians to better serve patients and make treatment decisions

[177LU]-LUPSMA

Partnered with PSMA-directed PETCT scan, LuPSMA offers a **Theranostic approach** to treatment of metastatic castration-resistant prostate cancer (mCRPC)

FOR PET/CT FINANCIAL ASSISTANCE:

PET/CT PATIENT SUPPORT

+63 998 323 5425
+63 917 714 4248
+63 917 714 4266
patientsupport@khealthcorp.com

aspen
PHILIPPINES

Levothyroxine sodium

Eltroxin

Thiamazole

Strumazol

aspen
PHILIPPINES
Healthcare. We Care.

Unit 1001-1002, 10th Floor
Trade and Financial Tower
7th Avenue cor. 32nd Street
Bonifacio Global City, Taguig City

Before prescribing, please review the Full Product Information available upon request from Aspen Philippines.
For product inquiries, concerns & suspected adverse drug reactions, email us at APH.PV.Phils@PH.Aspenpharma.com or call us at (02)7792-8000 / (0916)794 -9337

MESSIAH R4200

OPTIMIZED PERFORMANCE

USER-FRIENDLY PROGRAM

EFFICIENT & FLEXIBLE

KEY FEATURES

- DIFFERENT MODULES TO INSERT & MODIFY TESTS
- WORKLIST
- TIME MANAGEMENT SYSTEM
- QUALITY CONTROL PROGRAM
- WASHABLE DISPENSING NEEDLES
- LIQUID AND CLOT DETECTOR
- BARCODE READING SYSTEM

FULLY AUTOMATED OPEN SYSTEM INSTRUMENT FOR RIA TESTING

ARE YOU PREPARED FOR *THERANOSTICS?*

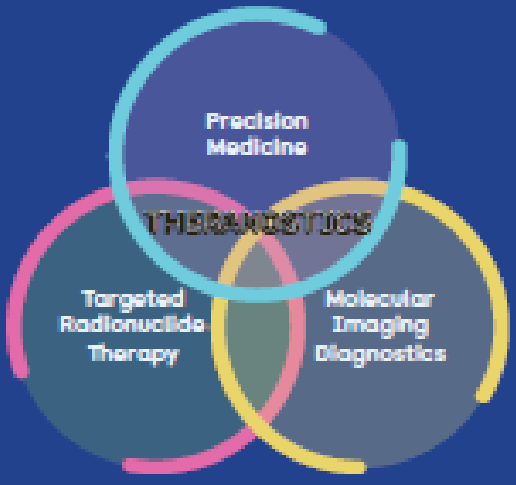

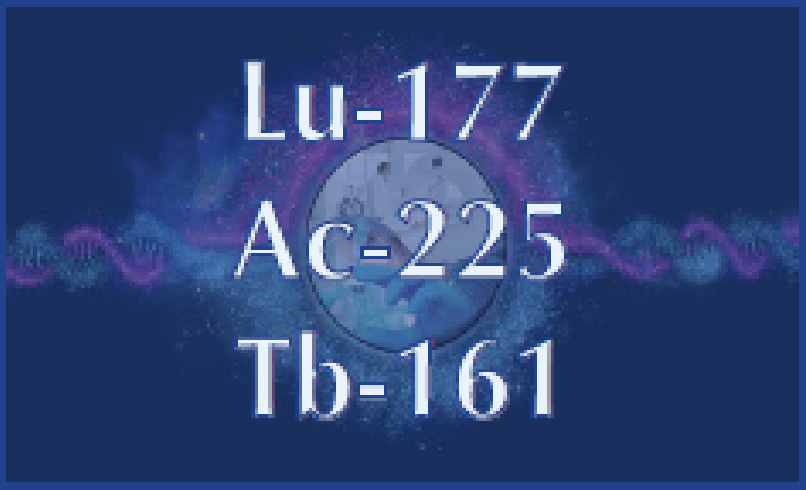

ASSURANCE CONTROLS TECHNOLOGIES CO., INC.
https://www.assurancecontrol.com/

OFFERING SOON

GE HealthCare

Connecting Every Step in Molecular Medicine

A Vision for Molecular Medicine.

DISCOVERY	DIAGNOSIS	TREATMENT
for development of **targeted** tracers and therapy	with **breakthrough** PET and SPECT imaging solutions	using **predictive** and advanced monitoring tools

We are focused on core challenges

At GE Healthcare we believe we can uniquely help connect the teams, data, and decisions in every step from discovery to diagnosis to treatment with intelligent efficient innovations that will ultimately help you deliver precise, personalized care. This is our vision.

There is so much data available across molecular imaging today. There are so many connection opportunities and loops to close. That's where we see significant opportunity. And we believe we're in a unique position to fulfill this vision because we are the only vendor with pharmaceutical diagnostics, cyclotrons, chemistry synthesis, PET/CT, SPECT/CT, advanced digital solutions and pharma partnerships to cover the breadth of steps from discovery to treatment.

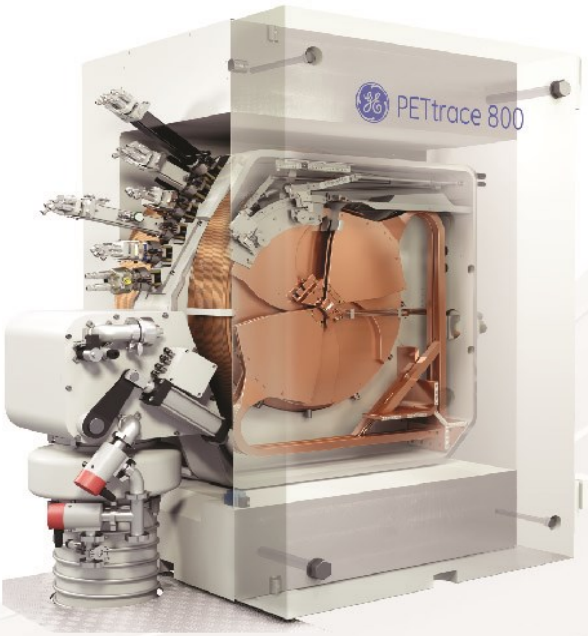

Please contact your local GE Healthcare representative to learn more or visit https://www.gehealthcare.com.sg/